Alexandros A. Taflanidis[1]
Department of Civil Engineering and Geological Sciences,
University of Notre Dame,
Notre Dame, IN 46556
e-mail: a.taflanidis@nd.edu

Jeffrey T. Scruggs
Department of Civil and Environmental Engineering,
Duke University,
Durham, NC 27708
e-mail: jeff.scruggs@duke.edu

James L. Beck
Engineering and Applied Science Division,
California Institute of Technology,
Pasadena, CA 91125
e-mail: jimbeck@caltech.edu

Robust Stochastic Design of Linear Controlled Systems for Performance Optimization

This study discusses a robust controller synthesis methodology for linear, time invariant systems, under probabilistic parameter uncertainty. Optimization of probabilistic performance robustness for $\mathcal{H}_2$ and multi-objective $\mathcal{H}_2$ measures is investigated, as well as for performance measures based on first-passage system reliability. The control optimization approaches proposed here exploit recent advances in stochastic simulation techniques. The approach is illustrated for vibration response suppression of a civil structure. The results illustrate that, for problems with probabilistic uncertainty, the explicit optimization of probabilistic performance robustness can result in markedly different optimal feedback laws, as well as enhanced performance robustness, when compared to traditional "worst-case" notions of robust optimal control. [DOI: 10.1115/1.4001849]

1 Introduction

In engineering design, the knowledge about a system is never complete. For an efficient and reliable design, all uncertainties involving the state of the system as well as the characteristics of future excitations should be explicitly treated. In many cases, a probability logic approach constitutes the most rational and consistent framework for quantifying all such uncertainties [1]. This is established by characterizing the relative plausibility of different properties of the system by probability models. The system performance is then quantified by measures, which reflect these probability models. When such a design process deals with probability models for system parameters (in addition, possibly, to input uncertainty), the robust design problem is called *robust stochastic design* [2,3], where the term robustness pertains to the stochastic, i.e., probabilistic, model description.

Most standard tools for robust control design, such as $\mathcal{H}_\infty$, μ-synthesis [4], and the many offshoots of these, consider a compact set of possible models for the system. Furthermore, analytical tractability often requires uncertainty to be modeled with less structure than is actually present, leading to an overconservative characterization of parameter variability [5]. Even when parametric uncertainty can be structured without conservativeness, no regard is given to the physical interpretation of the plant variations. Information implying that some model parameters are more probable than others is not explicitly treated. However, in most real engineering applications, there is considerable knowledge about the relative plausibility of these parameters. Furthermore, in many applications, the domain of *possible* model parameter values for a system can be extremely large and the selection of boundaries to ensure a compact set is quite arbitrary. However, subdomains of high relative *plausibility* are often concentrated and of much smaller size. In such circumstances, the notion of robustness can only be justifiably treated in a probabilistic framework rather than through worst-case (WC) or game-theoretic notions. Application of the aforementioned controller synthesis methodologies, therefore, typically leads to conservative designs, which may be inefficiently robust to real world uncertainties. Sometimes, this may be deemed acceptable from the point of view of stability robustness, especially when the instability of the closed-loop system might lead to catastrophic failures, which must be avoided at all expense no matter how conservative. However, when focus of the design is *robust performance* rather than simply *robust stability*, the aforementioned approaches may be lead to suboptimal design decisions, and possibly may lead to paralysis in design.

This observation has motivated a number of studies that investigate the stability and performance of controlled systems under probabilistic parameter uncertainty. The idea is to optimize *statistics* of the objective function (probabilistic performance) under plant uncertainty rather than the objective function resulting from the nominal model (nominal performance). The methods proposed in Refs. [3,6–8] characterize the probabilistically robust utility of a controller in terms of the probabilities of unacceptable closed-loop response either related to its stability or performance. The design objective was expressed as a weighted sum of these probabilities and evolutionary algorithms were proposed for performing the optimization for the controller parameters. Boers and coworkers [9,10] discussed the expected performance related to the $\mathcal{H}_2$ norm of the closed-loop system. These studies showed that the associated design problem is well-posed but they restricted their attention to a relatively simple subclass of parametric model uncertainty characterizations. Field et al. [11] focused on the probability of instability for controlled systems and used first-order reliability calculations to approximate it. The concept of first-passage system reliability under stochastic excitation has also been used as a design objective for control applications, expressed by the probability that the response output will not exit some region that defines acceptable performance. This approach was investigated in Ref. [12] for systems with probabilistic parameter uncertainty and stochastic excitation and further elaborated in Ref. [13]. Theoretical issues associated with this problem were recently investigated in Ref. [14], including its connections to other optimal control problems.

The present paper focuses on the robust design optimization of linear time invariant dynamical systems with probabilistically described parametric model uncertainties. We focus on control systems that involve a stochastic disturbance input. We consider $\mathcal{H}_2$ and multi-objective $\mathcal{H}_2$ control synthesis for quantification of the system nominal performance. The probabilistic measure of optimality is then defined either as the average (i.e., expectation) of the performance over the uncertain parameter space, or the probability that the performance will exceed acceptable bounds. We also examine robust stochastic design for minimal first-passage

[1]Corresponding author.

Contributed by the Dynamic Systems Division of ASME for publication in the JOURNAL OF DYNAMIC SYSTEMS, MEASUREMENT, AND CONTROL. Manuscript received November 5, 2009; final manuscript received May 3, 2010; published online August 19, 2010. Assoc. Editor: YangQuan Chen.

failure probability. In this case the definition of robust performance in the presence of probabilistic model uncertainties follows directly from the axioms of probability logic. Efficient analysis and synthesis methodologies are discussed, which are based on recently developed stochastic simulation techniques.

This paper makes several contributions. First, it discusses an efficient stochastic optimization framework for the controller synthesis. Second, it sheds light on differences between the first-passage reliability-based design and $\mathcal{H}_2$, or multi-objective $\mathcal{H}_2$ control designs, and on appropriate characterization of the probabilistic performance for the latter two. Third, it draws comparisons between probabilistically robust control design and more common "worst-case" interpretation of robustness. Finally, it examines the influence of different probability models on the optimal controller obtained through this design process, taking into account the physical connection between these models in describing the system uncertainty.

2 Problem Definition

We assume a linear dynamical state space model with state vector $\mathbf{x}(t) \in \mathbb{R}^{n_x}$ for which the dynamic system coefficients depend on uncertain parameters $\boldsymbol{\theta} \in \mathbb{R}^{n_\theta}$, i.e.,

$$\dot{\mathbf{x}}(t) = \mathbf{A}(\boldsymbol{\theta})\mathbf{x}(t) + \mathbf{B}(\boldsymbol{\theta})\mathbf{u}(t) + \mathbf{E}(\boldsymbol{\theta})\mathbf{w}(t)$$

$$\mathbf{z}(t) = \mathbf{C}(\boldsymbol{\theta})\mathbf{x}(t) + \mathbf{D}(\boldsymbol{\theta})\mathbf{u}(t)$$

$$\mathbf{y}(t) = \mathbf{L}(\boldsymbol{\theta})\mathbf{x}(t) \tag{1}$$

where $\mathbf{u}(t) \in \mathbb{R}^{n_u}$ is the control input and $\mathbf{y}(t) \in \mathbb{R}^{n_y}$ is the feedback output. The performance of the controlled system is assessed through $\mathbf{z}(t) \in \mathbb{R}^{n_z}$, the components of which are referred to as performance variables. Disturbance input $\mathbf{w}(t) \in \mathbb{R}^{n_a}$ is a zero-mean Gaussian white-noise vector process with spectral intensity matrix $\mathbf{I}$. We assume linear static feedback, i.e.,

$$\mathbf{u}(t) = \mathbf{K}(\boldsymbol{\varphi})\mathbf{y}(t) \tag{2}$$

where $\mathbf{K} \in \mathbb{R}^{n_u} \times \mathbb{R}^{n_y}$ and $\boldsymbol{\varphi} \in \Phi$ denotes the free parameters, which constitute the design variables of the problem. The image of Φ under $\mathbf{K}$ is denoted as $\mathcal{K}$.

In the course of this paper, we will discuss and establish a distinction between the system's *nominal* and *probabilistic performance*. The nominal performance is conditioned on a chosen nominal value of the parameter vector $\boldsymbol{\theta}$ and, thus, is always parameterized by a presumed $\boldsymbol{\theta}$ value. On the other hand, probabilistic performance utilizes a probability distribution for $\boldsymbol{\theta}$ and evaluates some statistical representation of the performance measure over this distribution. However, both the nominal and probabilistic performance measures are evaluated for a stochastic characterization of $\mathbf{w}$. The optimization of probabilistic performance with respect to the design variables is defined as *robust probabilistic design* or *robust stochastic design* with the term "stochastic" referring here to the probabilistic (i.e., stochastic) description for $\boldsymbol{\theta}$, as in Refs. [2,3]. In this context, the optimization of nominal performance is referred to as *nominal design*.

The nominal performance measure will be denoted $J(\mathbf{K}|\boldsymbol{\theta})$. For the controlled system under stationary stochastic disturbance in Eq. (1), two well motivated metrics that arise in many theoretical and practical control problems for characterizing this nominal performance are the $\mathcal{H}_2$ and multi-objective $\mathcal{H}_2$ measures, i.e.,

$$J_{\mathcal{H}_2}(\mathbf{K}|\boldsymbol{\theta}) = E\left\{ \lim_{T\to\infty} \frac{1}{T} \int_0^T \mathbf{z}(t)^T \mathbf{z}(t) dt \,|\boldsymbol{\theta} \right\} \tag{3}$$

$$J_{m\mathcal{H}_2}(\mathbf{K}|\boldsymbol{\theta}) = E\left\{ \max_{1\le i\le n_z} \left(\lim_{T\to\infty} \frac{1}{T} \int_0^T z(t)_i^2 dt \right) |\boldsymbol{\theta} \right\} \tag{4}$$

where $E\{.\}$ denotes expectation, with respect to $\mathbf{w}$, given $\boldsymbol{\theta}$.

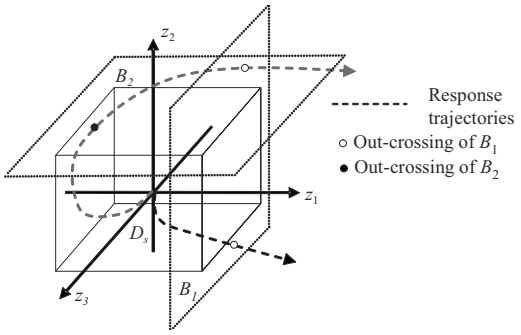

Fig. 1 Three-dimensional example of failure surfaces

Another appropriate performance measure is the first-passage system reliability, quantified as the probability that the output will not exceed acceptable thresholds. For linear system design these bounds define a hypercubic safe region $D_s \subset \mathbb{R}^{n_z}$.

$$D_s = \{\mathbf{z}(t) \in \mathbb{R}^{n_z} : |z_i(t)| < \gamma, \quad \forall\, i = 1, \ldots, n_z\} \tag{5}$$

Scaling factor $\gamma \in \mathbb{R}^+$ is used to uniformly vary the relationship of $\mathbf{z}$ to these thresholds. Figure 1 shows an example of D_s for a three-dimensional space. The optimal first-passage reliability controller is the one that minimizes the probability of unacceptable performance over some time duration $t \in [0, T]$, chosen to correspond to the duration of the event causing the dynamic excitation of the system. This conditional probability $P_F(\mathbf{K}|T, \boldsymbol{\theta})$ associated with controller $\mathbf{K}$ is commonly referred to as the (nominal) probability of failure and is defined as

$$J_F(\mathbf{K}|T, \boldsymbol{\theta}) = P_F(\mathbf{K}|T, \boldsymbol{\theta}) = P(\mathbf{z}(t) \notin D_s \text{ for some } t \in [0, T]) \tag{6}$$

3 Nominal Design

Assuming $\boldsymbol{\theta}$ is known, stationarity of system (1) under feedback (2) produces a zero-mean Gaussian distribution for $\mathbf{x}$ with covariance matrix $\boldsymbol{\Phi} = E[\mathbf{x}\mathbf{x}^T]$ determined by

$$[\mathbf{A}(\boldsymbol{\theta}) + \mathbf{B}(\boldsymbol{\theta})\mathbf{K}\mathbf{L}(\boldsymbol{\theta})]\boldsymbol{\Phi} + \boldsymbol{\Phi}[\mathbf{A}(\boldsymbol{\theta}) + \mathbf{B}(\boldsymbol{\theta})\mathbf{K}\mathbf{L}(\boldsymbol{\theta})]^T + \mathbf{E}(\boldsymbol{\theta})\mathbf{E}(\boldsymbol{\theta})^T = \mathbf{0} \tag{7}$$

The performance output $\mathbf{z}$ is then Gaussian-distributed with zero-mean and covariance

$$\boldsymbol{\Sigma}_{zz} = E\{\mathbf{z}(t)\mathbf{z}^T(t)\} = [\mathbf{C}(\boldsymbol{\theta}) + \mathbf{D}(\boldsymbol{\theta})\mathbf{K}\mathbf{L}(\boldsymbol{\theta})]\boldsymbol{\Phi}[\mathbf{C}(\boldsymbol{\theta}) + \mathbf{D}(\boldsymbol{\theta})\mathbf{K}\mathbf{L}(\boldsymbol{\theta})]^T \tag{8}$$

Thus, the performance objectives in Eqs. (3) and (4) are

$$J_{\mathcal{H}_2}(\mathbf{K}|\boldsymbol{\theta}) = \sum_{i=1}^{n_z} \sigma_{z_i}^2, \quad J_{m\mathcal{H}_2}(\mathbf{K}|\boldsymbol{\theta}) = \max_{1\le i\le n_z} (\sigma_{z_i}^2) \tag{9}$$

where $\sigma_{z_i}^2 = \{\boldsymbol{\Sigma}_{zz}\}_{ii}$.

The $\mathcal{H}_2$ and multi-objective $\mathcal{H}_2$, denoted as $m\mathcal{H}_2$, optimal static controllers are given, respectively, by

$$\mathbf{K}^*_{\mathcal{H}_2} = \arg\min_{\mathbf{K}\in\mathcal{K}} \left\{ \sum_{i=1}^{n_z} \sigma_{z_i}^2 \right\}, \quad \mathbf{K}^*_{m\mathcal{H}_2} = \arg\min_{\mathbf{K}\in\mathcal{K}} \{ \max_{1\le i\le n_z} \{\sigma_{z_i}^2\} \} \tag{10}$$

While these optimizations are in general nonconvex, output feedback controller synthesis problems have historically attracted considerable attention. Local optima can be solved iteratively, via Levine–Athans type algorithms [15] (for the standard $\mathcal{H}_2$ measure), and via various gradient-based algorithms [16]. More recently, matrix-inequality approaches have been proposed such as those involving branch-and-bound methods [17] and "convexi-

fied" LMI methods [18]. In general, the least tractable part of the problem is finding an initial stabilizing solution. However, if the nominal system is open-loop stable, as it is in the example considered in this paper, the identification of a stabilizing $\mathbf{K}$ is trivial (i.e., $\mathbf{K}=\mathbf{0}$).

The nominal probability of failure in Eq. (6) may be expressed as

$$P_F(\mathbf{K}|T,\boldsymbol{\theta}) = 1 - \exp(-\nu_{\mathbf{z}}^{+}(\mathbf{K}|\boldsymbol{\theta})T) \tag{11}$$

where the hazard function $\nu_{\mathbf{z}}^{+}(\mathbf{K}|\boldsymbol{\theta})$ is an approximation to the mean out-crossing rate of the boundary S_D of the safe region D_S conditioned on no previous out-crossing having occurred [19]:

$$\nu_{\mathbf{z}}^{+}(\mathbf{K}|\boldsymbol{\theta}) = \lim_{t\to\infty}\lim_{\Delta t\to 0}\frac{E[\text{number of out-crossings in } [t,t+\Delta t] \text{ of } D_S|\text{no out-crossings in } [0,t]]}{\Delta t} \tag{12}$$

This out-crossing rate $\nu_{\mathbf{z}}^{+}(\mathbf{K}|\boldsymbol{\theta})$ may be expressed as a sum of the out-crossing rates corresponding to each failure mode i:

$$\nu_{\mathbf{z}}^{+}(\mathbf{K}|\boldsymbol{\theta}) \approx \sum_{i=1}^{n_z} r_{z_i}^{+}\theta_{z_i}\lambda_{z_i} \tag{13}$$

where the dependence of the right hand side factors on $\mathbf{K}$ and $\boldsymbol{\theta}$ is omitted herein for notational simplicity. In this expression, $r_{z_i}^{+}$ is Rice's unconditional out-crossing rate, which accounts for out-crossing over the entire pair of hyperplanes $B_i=\{|z_i|=\gamma\}$ corresponding to failure mode i. Then, θ_{z_i} is a factor which accounts for spatial correlation between the different failure modes (out-crossings at different planar surfaces of S_D). Figure 1 illustrates this concept. Both trajectories in the figure correspond to "failure" for $z_1(t)$ but for the gray trajectory, the failure of z_2 precedes the failure of z_1 and so its failure is already accounted for as an out-crossing of $z_2=\gamma$ hyperplane. Rice's out-crossing rate does not distinguish between these two instances of out-crossing of the $z_1=\gamma$ hyperplane and the correlation weighting factors θ_{z_i} are introduced in Eq. (13) to account for this. Finally, λ_{z_i} is a correction factor, which accounts for correlation in time between out-crossings. This factor is important only for narrow-band systems or systems with small threshold definitions γ [19]. The detailed expressions for these factors are provided in Appendix A.

The first-passage reliability optimal controller is finally equivalent to the minimization of the stationary out-crossing rate $\nu_{\mathbf{z}}^{+}$ and the dependence on the time horizon T vanishes:

$$\mathbf{K}_F^{*} = \arg\min_{\mathbf{K}\in\mathcal{K}}(1-\exp(-\nu_{\mathbf{z}}^{+}(\mathbf{K}|\boldsymbol{\theta})T)) = \arg\min_{\mathbf{K}\in\mathcal{K}}(\nu_{\mathbf{z}}^{+}(\mathbf{K}|\boldsymbol{\theta})) \tag{14}$$

This is a nonlinear-nonconvex optimization problem that can be solved by any appropriate numerical technique. Algorithmic details about this optimization are discussed in Refs. [14,20].

An important question, so that design (14) is well motivated, is how it compares with other, more straight-forward optimal control problems discussed in literature. For answering this question, the different factors of $\nu_{\mathbf{z}}^{+}$ need to be analyzed from a controller optimization point of view. The principal component of $\nu_{\mathbf{z}}^{+}$ is Rice's out-crossing rate $r_{z_i}^{+}$ since it is directly related to the "failure events." This rate is a product of the factor $\exp\{-\gamma^2/(2\sigma_{z_i}^2)\}$, which increases with σ_{z_i}, and the factor $\sigma_{\dot{z}_i}/\sigma_{z_i}$, which increases with the bandwidth of z_i. The sensitivity of $\nu_{z_i}^{+}$ to changes in σ_{z_i} is much greater than to the ratio $\sigma_{\dot{z}_i}/\sigma_{z_i}$ because the variance enters into the equation as an exponential. The correlation weighting factor θ_{z_i} is also potentially significant because it accounts for correlation between different failure modes. For example, if failure mode 1 is only likely to occur if failure mode 2 has already occurred, then the statistics of failure mode 1 do not significantly affect P_F. Consequently, the assumption of uncorrelated failure events may lead to a significant departure from the true optimum. The influence of λ_{z_i} is generally less significant since this factor is only important for problems involving narrow-band systems or cases where even the optimal $\mathbf{K}^{*}$ results in frequent failures. Both these instances do not usually occur in practical control applications.

Considering these features, it was argued in Ref. [14] that for controller synthesis, the exponential-weighted term $(\gamma/\sigma_{z_i})^2$ is the most relevant factor of $\nu_{z_i}^{+}$ and that ultimately the out-crossing rate may be treated as a weighted sum of exponentials involving the reciprocal of the variances of each performance variable. This feature indicates a relationship of first-passage reliability design to $\mathcal{H}_2$ and $m\mathcal{H}_2$ designs. The exponential weighting gives greater importance to performance variables with larger variances, a characteristic which indicates a closer connection to $m\mathcal{H}_2$ design rather than $\mathcal{H}_2$ design. For $\gamma\to\infty$, $\forall i$, which means $\sigma_{z_i}/\gamma\to 0$, $\forall i$, the largest variance σ_{z_i} it the one that dominates the sensitivity of the out-crossing rate to each of the performance variable and $\mathbf{K}_F^{*}$ converges to the gain that minimizes this variance. $\mathbf{K}_F^{*}$ is, therefore, expected to be close to $\mathbf{K}_{m\mathcal{H}_2}^{*}$ when extremely rare events are considered for the system failure performance. If more than one performance variable is equally important in this setting, then their relative significance will be decided by their "weighting coefficients" with emphasis on the bandwidth factor (since the spatial and time correlation corrections are expected to be similar for such variables). For values of γ that do not focus on such rare events, notable differences may exist between first-passage reliability and $m\mathcal{H}_2$ synthesis, as will be shown later.

4 Robust Stochastic Design

4.1 Robust Stochastic Model Description. Let $\Theta\subset\mathbb{R}^{n_\theta}$ denote the domain of possible values of the model parameters $\boldsymbol{\theta}$ for the model class chosen to represent the system. Some of these values may be more probable than others. This relative plausibility of different model parameter values constitutes prior knowledge about the system and can be quantified by assigning a probability density function (PDF) $p(\boldsymbol{\theta})$ [1].

Nonparametric modeling uncertainty may also be addressed by introducing a model prediction error, i.e., an error between the response of the actual system and the response of the model adopted for it. This prediction error may be modeled probabilistically [21] and augmented into the uncertain parameter vector $\boldsymbol{\theta}$. It addresses the fact that no mathematical model can exactly describe the behavior of a physical system; as such, it quantifies the uncertainty for the model set selected for representing the system.

The specific probability model for the model parameters $\boldsymbol{\theta}$ should be based on the available prior knowledge about them and should not spuriously reduce the uncertainty corresponding to

these parameters beyond that which is supported by this knowledge. This is established by choosing probability models that maximize the amount of uncertainty about the parameter values, as quantified by Shannon's information entropy [22] for the parameter probability model $p(\boldsymbol{\theta})$, subject to chosen constraints for the statistics of $\boldsymbol{\theta}$ based on prior knowledge about the system. For a continuous parameter vector $\boldsymbol{\theta}$ with PDF $p(\boldsymbol{\theta})$, the information entropy is given by

$$E_p = -\int_{\Theta} p(\boldsymbol{\theta})\log_2(p(\boldsymbol{\theta}))d\boldsymbol{\theta} \tag{15}$$

This selection of probability models as state-of-knowledge models that maximize the amount of uncertainty about the parameters subject to constraints is the principle of maximum (Shannon) entropy, which was first proposed by Jaynes in 1957 [1]. Selection of any other probability model would reduce the amount of uncertainty without specifying additional information so the choice would be open to justified criticism. For example, for a continuous uncertain variable on a compact domain with specified mean and variance, the most appropriate probability model selection (i.e., the one that maximizes the entropy) is a Gaussian PDF that is truncated so that its support is the domain. On the other hand, if no specifications are made of any moments of the distribution then the most appropriate probability model is a uniform distribution over the domain.

In this robust probabilistic setting for the system model description, the overall performance is defined by appropriate probabilistic measures that exploit the available system model information. This performance quantification is discussed next. The associated controller optimization problem is then addressed in Sec. 5.

4.2 Robust Performance: General Case. The robust-performance quantification requires the extension of the nominal performance $J(\mathbf{K}|\boldsymbol{\theta})$ to a probabilistic one $H(\mathbf{K})$. This quantification can be established in various ways but in general will be quantified by a stochastic integral of the form

$$H(\mathbf{K}) \triangleq E_{\boldsymbol{\theta}}[j(\mathbf{K}|\boldsymbol{\theta})] = \int_{\Theta} j(\mathbf{K}|\boldsymbol{\theta})p(\boldsymbol{\theta})d\boldsymbol{\theta} \tag{16}$$

where $E_{\boldsymbol{\theta}}[.]$ denotes expectation over the uncertain parameter space and the loss function $j(\mathbf{K}|\boldsymbol{\theta})$ is related to the deterministic performance measure $J(\mathbf{K}|\boldsymbol{\theta})$. We assume here that the chosen probability model for $\boldsymbol{\theta}$ does not depend on the controller design, otherwise $p(\boldsymbol{\theta})$ should be replaced by $p(\boldsymbol{\theta}|\mathbf{K})$ (no additional modifications are then needed in the proposed approach). By appropriate definition of $j(\mathbf{K}|\boldsymbol{\theta})$, different probabilistic measures $H(\mathbf{K})$ can be quantified. The probabilistically robust controller is then given by the optimization

$$\mathbf{K}^* = \arg\min_{\mathbf{K}\in\mathcal{K}} \int_{\Theta} j(\mathbf{K}|\boldsymbol{\theta})p(\boldsymbol{\theta})d\boldsymbol{\theta} \tag{17}$$

where the convention is that lower values of $j(\mathbf{K}|\boldsymbol{\theta})$ correspond to better performance.

In the present work we will focus on two basic choices for $H(\mathbf{K})$: (a) the probabilistic average value of $J(\mathbf{K}|\boldsymbol{\theta})$ or (b) the probability that $J(\mathbf{K}|\boldsymbol{\theta})$ will exceed some acceptable threshold. These performance measures (and their resultant optimal designs) will be called *average robustness* (AR) and *reliability-robustness* (RR) measures (designs), respectively. Their objective functions are

$$\text{AR: } H_{\text{AR}}(\mathbf{K}) \triangleq E_{\boldsymbol{\theta}}[J(\mathbf{K}|\boldsymbol{\theta})] = \int_{\Theta} J(\mathbf{K}|\boldsymbol{\theta})p(\boldsymbol{\theta})d\boldsymbol{\theta} \tag{18}$$

$$\text{RR: } H_{\text{RR}}(\mathbf{K}) \triangleq P(J(\mathbf{K}|\boldsymbol{\theta}) > b|\mathbf{K}) = E_{\boldsymbol{\theta}}[I_b(\mathbf{K}|\boldsymbol{\theta})] = \int_{\Theta} I_b(\mathbf{K}|\boldsymbol{\theta})p(\boldsymbol{\theta})d\boldsymbol{\theta} \tag{19}$$

where the *indicator function* $I_b(\mathbf{K}|\boldsymbol{\theta})$ is

$$I_b(\mathbf{K}|\boldsymbol{\theta}) = \begin{cases} 1 & : \quad J(\mathbf{K}|\boldsymbol{\theta}) > b \\ 0 & : \quad J(\mathbf{K}|\boldsymbol{\theta}) \le b \end{cases} \tag{20}$$

An equivalent characterization of reliability robust performance in Eq. (19) can be established by explicitly considering the influence of the model prediction error. Let $g_a(\mathbf{K})$ be the response quantity defining the failure of the actual system rather than the corresponding quantity for the system model, so that the conditional probability of failure is $P(J>b|\boldsymbol{\theta},\mathbf{K})=P(g_a>0|\boldsymbol{\theta},\mathbf{K})$ and let $g(\boldsymbol{\theta},\mathbf{K})$ be the limit state function defining the failure of the model in a similar way. If the model prediction error $\varepsilon(\boldsymbol{\theta},\mathbf{K})$ is defined so that

$$\varepsilon(\boldsymbol{\theta},\mathbf{K}) = g_a(\mathbf{K}) - g(\boldsymbol{\theta},\mathbf{K}) \tag{21}$$

with a PDF symmetric about zero then the integral in Eq. (19) can be transformed to [23]

$$P(J > b|\mathbf{K}) = \int_{\Theta} P_{\varepsilon}(g(\boldsymbol{\theta},\mathbf{K})|\boldsymbol{\theta},\mathbf{K})p(\boldsymbol{\theta})d\boldsymbol{\theta} \tag{22}$$

where $P_{\varepsilon}(.|\boldsymbol{\theta},\mathbf{K})$ is the cumulative distribution function for ε conditional on $\{\boldsymbol{\theta},\mathbf{K}\}$ and in this case vector $\boldsymbol{\theta}$ does not include the prediction error ε, whereas in Eq. (19) $\boldsymbol{\theta}$ corresponds to the augmented vector that includes ε. In formulation (22), $I_b(.)$ is replaced by $P_{\varepsilon}(.)$. Expressions Eqs. (19) and (22) are thus equivalent and either of them can be used as objective functions for RR design. The latter expression, however, reveals the influence of the model prediction error in this approach; this error may be equivalently regarded as introducing a smooth function $P_{\varepsilon}(g(\boldsymbol{\theta},\mathbf{K})|\boldsymbol{\theta},\mathbf{K})$ to reflect a preference for J, as opposed to the binary distinction imposed by the indicator function $I_b(\mathbf{K}|\theta)$.

Which of the two probabilistic performance quantifications (AR or RR) is more appropriate for control design is directly related to the nature of the metric $J(\mathbf{K}|\boldsymbol{\theta})$ and the criteria adopted in the design, i.e., which objective is more important—regulation of average performance, or avoidance of extreme performance. The most appropriate measure for $\mathcal{H}_2$ performance is AR since the $\mathcal{H}_2$ metric is related to the average response of the system. Such quantification has been discussed also in Refs. [9,10]. The first study presented a theoretical investigation and showed that the associated design problem is well-posed. The second discussed necessary and sufficient conditions for the optimal feedback gain but did not address issues related to the estimation of the associated stochastic integrals; it was rather restricted to simpler applications for the characterization of the parametric model uncertainty for which the calculation of these integrals is straight-forward. For the $m\mathcal{H}_2$ performance, both AR and RR could be appropriate, depending on the application. The probabilistic characterization of the $m\mathcal{H}_2$ performance does not seem to have received any special attention in control literature.

4.3 Robust Performance: First-Passage Reliability Design. For the first-passage reliability, the robust-performance definition follows directly from the basic principles of probability logic; the failure probability defined by the models characterized by $\boldsymbol{\theta}\in\boldsymbol{\Theta}$ with PDF $p(\boldsymbol{\theta})$ is expressed by the total probability theorem as

$$P_F(\mathbf{K}|T) = \int_\Theta P_F(\mathbf{K}|T,\boldsymbol{\theta})p(\boldsymbol{\theta})d\boldsymbol{\theta}$$

$$= 1 - \int_\Theta p(\boldsymbol{\theta})\exp(-\nu_{\mathbf{z}}^+(\mathbf{K}|\boldsymbol{\theta})T)d\boldsymbol{\theta}$$

$$= 1 - E_{\boldsymbol{\theta}}[\exp(-\nu_{\mathbf{z}}^+(\mathbf{K}|\boldsymbol{\theta})T)] \quad (23)$$

This defines the *robust first-passage failure probability*. Note that this characterization is equivalent to the average robustness definition.

The robust first-passage reliability controller optimization problem may be expressed as

$$\mathbf{K}_{\mathrm{FR}_c}^* = \arg\min_{\mathbf{K}\in\mathcal{K}}(P_F(\mathbf{K}|T))$$

$$= \arg\min_{\mathbf{K}\in\mathcal{K}}\left(1 - \int_\Theta p(\boldsymbol{\theta})\exp(-\nu_{\mathbf{z}}^+(\mathbf{K}|\boldsymbol{\theta})T)d\boldsymbol{\theta}\right) \quad (24)$$

Contrary to the nominal case, the choice of the time horizon T influences the design optimization. This duration can be interpreted as the finite time horizon associated with the optimal reliability control problem. To further characterize its influence on the optimization, consider a Taylor series expansion of Eq. (23). The robust first-passage failure probability and the associated optimal controller are then expressed by

$$P_F(\mathbf{K}|T) = -\sum_{j=1}^{\infty}\frac{(-T)^j}{j!}E_{\boldsymbol{\theta}}[(\nu_{\mathbf{z}}^+(\mathbf{K}|\boldsymbol{\theta}))^j] \quad (25)$$

$$\mathbf{K}_{\mathrm{FR}_c}^* = \arg\min_{\mathbf{K}\in\mathcal{K}}\left(-\sum_{j=1}^{\infty}\frac{(-T)^j}{j!}E_{\boldsymbol{\theta}}[(\nu_{\mathbf{z}}^+(\mathbf{K}|\boldsymbol{\theta}))^j]\right) \quad (26)$$

Thus, robust first-passage reliability design weighs the mean value of ν_z^+ (obtained for $j=1$ in the last infinite sum) against its higher-order moments over the uncertain parameter space. Time horizon T enters the problem as a sensitivity parameter, which defines the relative importance of the higher-order statistics. For small time horizons, the optimal robust-reliability controller is the one that minimizes the expected value of the out-crossing rate, evaluated over the uncertain parameter space without considering the higher-order statistics. As T increases, the higher-order moments become important.

For large T, Taflanidis et al. [14] used an asymptotic approximation around the global optimum of the integrand to produce the following approximate result:

$$\mathbf{K}_{\mathrm{FR}_c}^*|_{T\to\infty} = \arg\min_{\mathbf{K}\in\mathcal{K}}\{\nu_{\mathbf{z}}^+(\mathbf{K}|\boldsymbol{\theta}^*)\}$$

$$\boldsymbol{\theta}^*|_{T\to\infty} = \arg\min_{\boldsymbol{\theta}\in\boldsymbol{\Theta}}\{\nu_{\mathbf{z}}^+(\mathbf{K}_{\mathrm{FR}_c}^*|\boldsymbol{\theta})\} \quad (27)$$

Thus, the controller optimization seeks to improve the dynamic performance in regions of Θ for which the out-crossing rate is small. This design goal is in contrast to the usual objectives of robust design because it focuses on regions of the uncertain parameter space for which regulation of the response is not so important, i.e., where the out-crossing rate is small without regard to the plausibility of the models that these regions represent. One could, perhaps, view this outcome as being because failure is so likely for all $\boldsymbol{\theta}\in\Theta$ that the optimization concentrates on the value of $\boldsymbol{\theta}$ that provides the "last, best hope" of preventing failure, irrespective of the likelihood of this parameter vector.

This discussion shows that choice of T must therefore be made with some care. A logical assumption is to take T as the duration of the dynamic excitation, depending on the purpose of the control system, which suggests that it should be also treated as an uncertain parameter. If only the mean duration $\bar{T}$ is specified, then the most appropriate probability model for T, based on Jaynes' principle of maximum entropy, is an exponential distribution, i.e.,

$$p(T) = \begin{cases} \frac{1}{\bar{T}}\exp\left(-\frac{T}{\bar{T}}\right) & T>0 \\ 0 & T\le 0 \end{cases} \quad (28)$$

The probability of failure may be then calculated as

$$P_F(\mathbf{K}|\bar{T}) = \int_\Theta\int_0^\infty P_F(\mathbf{K}|T,\boldsymbol{\theta})p(\boldsymbol{\theta})p(T)dTd\boldsymbol{\theta}$$

$$= 1 - \int_\Theta \frac{p(\boldsymbol{\theta})}{\nu_{\mathbf{z}}^+(\mathbf{K}|\boldsymbol{\theta})\bar{T}+1}d\boldsymbol{\theta} \quad (29)$$

and the robust first-passage reliability optimal controller is

$$\mathbf{K}_{\mathrm{FR}}^* = \arg\min_{\mathbf{K}\in\mathcal{K}}\left(1 - \int_\Theta \frac{p(\boldsymbol{\theta})}{\nu_{\mathbf{z}}^+(\mathbf{K}|\boldsymbol{\theta})\bar{T}+1}d\boldsymbol{\theta}\right) \quad (30)$$

We will denote this case by FR, whereas the first-passage reliability controller when T is treated as certain is denoted by FR_c.

Employing a Taylor series expansion in this case leads to the following results. For small $\bar{T}$, we can assume that $\nu_{\mathbf{z}}^+\bar{T}<1$ $\forall\,\boldsymbol{\theta}\in\Theta$, which leads to

$$P_F(\mathbf{K}|\bar{T}) = -\sum_{j=1}^{\infty}(-\bar{T})^j E_{\boldsymbol{\theta}}[(\nu_{\mathbf{z}}^+(\mathbf{K}|\boldsymbol{\theta}))^j] \quad (31)$$

On the other hand for large $\bar{T}$, we can assume that $\nu_{\mathbf{z}}^+\bar{T}>1$ $\forall\,\boldsymbol{\theta}\in\Theta$, which leads to

$$P_F(\mathbf{K}|\bar{T}) = 1 + \sum_{j=1}^{\infty}(-\bar{T})^{-j} E_{\boldsymbol{\theta}}[(\nu_{\mathbf{z}}^+(\mathbf{K}|\boldsymbol{\theta}))^{-j}] \quad (32)$$

The first of these expansions leads to the conclusion that

$$\mathbf{K}_{\mathrm{FR}|\bar{T}\to 0}^* = \arg\min_{\mathbf{K}\in\mathcal{K}}\{E_{\boldsymbol{\theta}}[\nu_{\mathbf{z}}^+(\mathbf{K}|\boldsymbol{\theta})]\} \quad (33)$$

This optimization is identical to the case for deterministic T with $T\to 0$. This is not surprising because T is being treated as probabilistic with an arbitrarily narrow distribution, thus converging to the deterministic case as $T\to 0$.

For the infinite time horizon we have that

$$\mathbf{K}_{\mathrm{FR}|\bar{T}\to\infty}^* = \arg\max_{\mathbf{K}\in\mathcal{K}}\{E_{\boldsymbol{\theta}}[\nu_{\mathbf{z}}^+(\mathbf{K}|\boldsymbol{\theta})^{-1}]\} \quad (34)$$

This expression has a very intuitive interpretation (contrary to the one in Eq. (27)). It is straight-forward to show that, for a given $\boldsymbol{\theta}\in\Theta$, the quantity $\nu_{\mathbf{z}}^+(\mathbf{K}|\boldsymbol{\theta})^{-1}$ is the expected (i.e., average) time duration between out-crossings in stationary response. Thus, the robust first-passage reliability optimal controller for the infinite time horizon case is the one that maximizes the expected time between out-crossings.

5 Stochastic Analysis and Optimization

In this section we discuss evaluation and optimization of the stochastic integrals encountered in the robust-performance quantification presented in the previous sections. We refer to these two tasks as *stochastic analysis* and *stochastic optimization*, respectively. The general form for all these integrals, expressed in terms of the design variables for the controller $\boldsymbol{\varphi}$ is

$$H(\mathbf{K}) = H(\boldsymbol{\varphi}) \triangleq E_{\boldsymbol{\theta}}[h(\boldsymbol{\varphi},\boldsymbol{\theta})] = \int_\Theta h(\boldsymbol{\varphi},\boldsymbol{\theta})p(\boldsymbol{\theta})d\boldsymbol{\theta} \quad (35)$$

for some appropriate selection of the performance function $h(\boldsymbol{\varphi},\boldsymbol{\theta}):\mathbb{R}^{n_\varphi}x\mathbb{R}^{n_\theta}\to\mathbb{R}^+$. The associated design optimization problem is then

$$\boldsymbol{\varphi}^* = \arg\min_{\boldsymbol{\varphi}\in\boldsymbol{\Phi}} H(\boldsymbol{\varphi}) \tag{36}$$

where we are considering without loss of generality, the minimization of the objective function.

If the dimension of $\boldsymbol{\theta}$ is large (typically larger than 2), the integral in Eq. (35) can only rarely be numerically evaluated. Many analytical approximations have been proposed for estimation of such stochastic integrals but they are not always guaranteed to converge to the actual optimal solution. The alternative approach, taken here, is to estimate the integral in Eq. (35) by stochastic simulation. Using a finite number N of random samples of $\boldsymbol{\theta}$ drawn from $p(\boldsymbol{\theta})$, an estimate for Eq. (35) is given by

$$\hat{H}(\boldsymbol{\varphi}) \triangleq \frac{1}{N}\sum_{i=1}^{N} h(\boldsymbol{\varphi}, \boldsymbol{\theta}_i) \tag{37}$$

where vector $\boldsymbol{\theta}_i$ denotes the sample of the uncertain parameters used in the ith simulation. The computational complexity for generating these samples depends on the probability model $p(\boldsymbol{\theta})$ but novel techniques have been recently developed [24,25], the best-known being Markov chain Monte Carlo (MCMC) [26], which have significantly improved the computational efficiency of this task. The notation $\hat{H}(\boldsymbol{\varphi}, \boldsymbol{\Omega}_N)$ is also used to explicitly denote the dependence of the estimate $\hat{H}$ on the sample set of the model parameters $\boldsymbol{\Omega}_N = [\boldsymbol{\theta}_1, \ldots, \boldsymbol{\theta}_N]$.

As $N \to \infty$, $\hat{H}(\boldsymbol{\varphi}) \to H(\boldsymbol{\varphi})$ but even for finite sufficiently large N, Eq. (37) gives a good approximation for Eq. (35) with a coefficient of variation (cov) decreasing proportional to $1/\sqrt{N}$ [24]. The value for N can be a priori selected based on appropriate bounds that depend on the required accuracy for the estimate in Eq. (37) (see, for example, the discussion in Ref. [27]) or can be adaptively adjusted during the optimization [28].

For improving the computational efficiency of the estimation for $H(\boldsymbol{\varphi})$, importance sampling (IS) may be used. This is established by introducing an importance sampling density $p_{\mathrm{IS}}(\boldsymbol{\varphi})$ to focus on regions of the Θ space that contribute more to the stochastic integral. An estimate for it is given in this case by

$$\hat{H}(\boldsymbol{\varphi}) \triangleq \frac{1}{N}\sum_{i=1}^{N} h(\boldsymbol{\varphi}, \boldsymbol{\theta}_i)\frac{p(\boldsymbol{\theta})}{p_{\mathrm{IS}}(\boldsymbol{\theta})} \tag{38}$$

where the samples $\boldsymbol{\theta}_i$ are simulated according to $p_{\mathrm{IS}}(\boldsymbol{\theta})$. If the importance sampling densities are appropriately selected then application of IS may lead to significant reduction of the cov of the estimate in Eq. (38) [24]; thus, accurate estimates of the objective function may be established using smaller values for N (and thus smaller computational effort). For example, efficient IS densities may be created if $p_{\mathrm{IS}}(\boldsymbol{\theta})$ is chosen to have its maxima in proximity to the same points as the maxima of the integrand but this requires an optimization to identify these design points at each iteration of the optimization algorithm that seeks $\boldsymbol{\varphi}^*$. Later in this paper, we describe another adaptive methodology for selecting $p_{\mathrm{IS}}(\boldsymbol{\theta})$.

The optimal design choice is finally given by the *stochastic optimization*:

$$\boldsymbol{\varphi}^* = \arg\min_{\boldsymbol{\varphi}\in\Phi} \hat{H}(\boldsymbol{\varphi}) \tag{39}$$

The estimate for the objective function for this optimization involves an unavoidable estimation error and significant computational cost since N evaluations of the model response are needed for each stochastic analysis, which make the optimization problem challenging. References [27,29,30] discuss appropriate optimization algorithms. Any of these algorithms may be used for solving problem (39). However, all of these algorithms require a large number of iterations, that is, a large number of stochastic analyses. A two-stage framework for performing the design optimization, which greatly reduces the number of iterations, is discussed next. In the first stage a novel method called stochastic subset optimization (SSO) [2] is applied for efficiently exploring the sensitivity of $H(\boldsymbol{\varphi})$ and identifying subsets of Φ that have high likelihood of containing the optimal design variables. In the second stage, the information available from SSO is used with any appropriate stochastic optimization algorithm to pinpoint more precisely the optimal design choice.

5.1 Stochastic Subset Optimization. The basic idea behind SSO is the formulation of an augmented stochastic problem, where the design variables are artificially considered as uncertain with uniform distribution $p(\boldsymbol{\varphi})$ over the design space Φ. In the context of this augmented stochastic design problem, we define the auxiliary PDF $\pi(\boldsymbol{\varphi}, \boldsymbol{\theta})$ as

$$\pi(\boldsymbol{\varphi}, \boldsymbol{\theta}) = \frac{h(\boldsymbol{\varphi}, \boldsymbol{\theta})p(\boldsymbol{\varphi}, \boldsymbol{\theta})}{E_{\boldsymbol{\varphi},\boldsymbol{\theta}}[h(\boldsymbol{\varphi}, \boldsymbol{\theta})]} \propto h(\boldsymbol{\varphi}, \boldsymbol{\theta})p(\boldsymbol{\varphi}, \boldsymbol{\theta}) \tag{40}$$

with $p(\boldsymbol{\varphi}, \boldsymbol{\theta}) = p(\boldsymbol{\varphi})p(\boldsymbol{\theta})$. The denominator of $\pi(\boldsymbol{\varphi}, \boldsymbol{\theta})$

$$E_{\boldsymbol{\varphi},\boldsymbol{\theta}}[h(\boldsymbol{\varphi}, \boldsymbol{\theta})] = \int_{\Phi}\int_{\Theta} h(\boldsymbol{\varphi}, \boldsymbol{\theta})p(\boldsymbol{\varphi}, \boldsymbol{\theta})d\boldsymbol{\theta}d\boldsymbol{\varphi} \tag{41}$$

is the expected value of utility function h over the augmented uncertain space and is not explicitly needed; it is simply a normalization constant. In the context of the augmented stochastic problem, the objective function $E_{\boldsymbol{\theta}}[h(\boldsymbol{\varphi}, \boldsymbol{\theta})]$ may be expressed as

$$E_{\boldsymbol{\theta}}[h(\boldsymbol{\varphi}, \boldsymbol{\theta})] = \frac{E_{\boldsymbol{\varphi},\boldsymbol{\theta}}[h(\boldsymbol{\varphi}, \boldsymbol{\theta})]}{p(\boldsymbol{\varphi})}\pi(\boldsymbol{\varphi}) \propto \pi(\boldsymbol{\varphi}) \tag{42}$$

where the marginal PDF $\pi(\boldsymbol{\varphi})$ is equal to

$$\pi(\boldsymbol{\varphi}) = \int_{\Theta} \pi(\boldsymbol{\varphi}, \boldsymbol{\theta})d\boldsymbol{\theta} \tag{43}$$

Since $E_{\boldsymbol{\varphi},\boldsymbol{\theta}}[h(\boldsymbol{\varphi}, \boldsymbol{\theta})]$ and $p(\boldsymbol{\varphi})$ are constants, the marginal PDF $\pi(\boldsymbol{\varphi})$ expresses the sensitivity of the objective function $E_{\boldsymbol{\theta}}[h(\boldsymbol{\varphi}, \boldsymbol{\theta})]$ with respect to the design variables. Samples of this PDF can be obtained through stochastic simulation techniques [2], for example, by direct Monte Carlo or Markov chain Monte Carlo sampling. These algorithms will give sample pairs $[\boldsymbol{\varphi}, \boldsymbol{\theta}]$ that are distributed according to the joint distribution $\pi(\boldsymbol{\varphi}, \boldsymbol{\theta})$, i.e., according to $h(\boldsymbol{\varphi}, \boldsymbol{\theta})p(\boldsymbol{\varphi}, \boldsymbol{\theta})$ when normalized. The $\boldsymbol{\varphi}$ component is obtained from samples from the marginal distribution $\pi(\boldsymbol{\varphi})$. A sensitivity analysis can be efficiently performed by exploiting the information in these samples. This is undertaken by identifying the subset $I \subset \Phi$ within some class A of admissible subsets, which has the smallest estimated average value of $E_{\boldsymbol{\theta}}[h(\boldsymbol{\varphi}, \boldsymbol{\theta})]$. The class of admissible subsets is defined by imposing appropriate geometrical and size constraints [2]. This leads to the *stochastic subset optimization*:

$$\hat{I} = \arg\min_{I\in A} N_I/V_I \tag{44}$$

where N_I is the number of samples in set I with volume V_I. This is a challenging optimization problem because it is nonsmooth due to the discontinuous relationship between I and the number of sample points it includes. However, the objective function can be calculated with small computational effort. As such, many candidate solutions can be explored at minimal computational cost and the optimization can be efficiently solved if an appropriate algorithm, for example, an algorithm based on direct search methodologies, is chosen [31].

Subset $\hat{I}$ in Eq. (44) has the highest likelihood within A of including $\boldsymbol{\varphi}^*$ in terms of the information available through the obtained samples. A measure of the quality of this identification is the estimated ratio of volume density of samples:

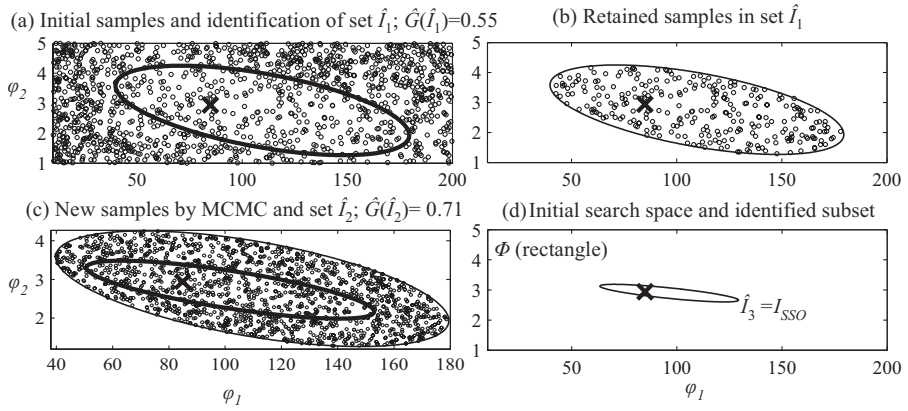

Fig. 2 Illustration of some key steps in SSO. The x in the plots corresponds to the optimal solution

$$\hat{G}(I) = \frac{N_I/V_I}{N_\Phi/V_\Phi} \tag{45}$$

which is equal to the ratio of the estimated average values for the objective function in sets I and Φ, respectively, [2]. Smaller values for this ratio correspond to larger likelihoods for $\hat{I}$ to include $\boldsymbol{\varphi}^*$ since they correspond to greater differences for the average value within $\hat{I}$ and Φ. On the other hand, a value for $\hat{G}(I)$ close to unity implies nearly the same average value for the objective function for subsets I and Φ; this case indicates that the search for the optimal I is challenging because the objective function is insensitive to the selection of I.

Instead of trying to identify a small region in one single step as above, the efficiency of the subset optimization can be increased if an iterative approach is adopted (see also Fig. 2). At iteration k, MCMC simulation is implemented in order to obtain additional samples in $\hat{I}_{k-1}$, each distributed according to $\pi(\boldsymbol{\varphi}, \boldsymbol{\theta})$, using the samples available from the previous iteration (see the discussion, which follows) as seeds for the generated Markov chains. The optimal region $\hat{I}_k \subset \hat{I}_{k-1}$ is then identified as described above with the only difference that the search domain is confined to $\hat{I}_{k-1}$. After identification of $\hat{I}_k$ only the samples whose $\boldsymbol{\varphi}$ components are in $\hat{I}_{k-1}$ are retained for the next iteration. These samples for $\boldsymbol{\varphi}$ and $\boldsymbol{\theta}$ are distributed proportional to the target sampling density $\pi(\boldsymbol{\varphi}, \boldsymbol{\theta})$, when $\boldsymbol{\varphi} \in \hat{I}_k$, and therefore can be used in the next iteration of the SSO algorithm to improve the efficiency of the stochastic sampling process. This can be established not only by using them as seeds for MCMC sampling, as discussed earlier but also by exploiting them to form better proposal densities in the MCMC approach [2,26]. Note that since the seeds for generating the Markov Chains, in this approach, already follow the target distribution, no burn-in period is required for the chains to reach stationarity.

For each iteration of the SSO algorithm, only a single stochastic analysis is required and, thus, the computational cost is comparable to the cost required for a single evaluation of the objective function in Eq. (38). But in SSO, information about the global behavior (over Φ) of the objective function is obtained. This is what contributes to the high efficiency of SSO compared to other stochastic optimization algorithms. Also, as long as optimization (44) can be efficiently performed, the computational cost of SSO increases only linearly with the dimension of the design variables when this iterative scheme is used [2].

More details about SSO, including discussion of the appropriate selection of the shape and size of the admissible subsets and the stopping criteria for the iterative process may be found in Ref. [2]. Applications that involve reliability integrals of form (19) are discussed in detail in Ref. [23]. The stopping criteria for SSO are not only related to the value for Eq. (45) but also to the desired accuracy or resolution of the identified solution. For the definition of admissible subsets the hyperellipses that contain a specific ratio of samples $A_\rho = \{I \subset \Phi : \rho = N_I/N_\Phi\}$ has been shown to be effective [2]. In this scheme, the size of the admissible subsets is adaptively chosen so that it includes a specific number of the simulated samples.

Figure 2 illustrates the key points of SSO as an optimization framework. In a small number of iterations, SSO adaptively converges to a subregion I_{SSO}, which contains $\boldsymbol{\varphi}^*$ and has small sensitivity with respect to $\boldsymbol{\varphi}$ (i.e., low $\hat{G}(I)$). I_{SSO} can also give information about the local behavior of the objective function near $\boldsymbol{\varphi}^*$, if there are admissible subsets with boundaries similar to the level surfaces of the objective function, i.e., if the chosen geometric shapes for the admissible subsets are similar to the shapes of the level surfaces.

5.2 Two-Stage Framework for Stochastic Optimization. When SSO has converged, all designs in I_{SSO} give nearly the same value of $H(\boldsymbol{\varphi})$ and so can be considered near-optimal. The center of the set I_{SSO}, $\boldsymbol{\varphi}_{SSO}$, can be taken as an approximation for $\boldsymbol{\varphi}^*$. There is, however, no rigorous measure of the quality of the identified solution, i.e., there is no guaranteed bound on $\|\boldsymbol{\varphi}_{SSO} - \boldsymbol{\varphi}^*\|$. If higher accuracy is required for the optimal design variables, a second optimization stage can be performed. Problem (39) should be solved in this second stage by exploiting *all information* available from SSO regarding the sensitivity with respect to both $\boldsymbol{\varphi}$ and $\boldsymbol{\theta}$. Either gradient-based or gradient-free algorithms (such as evolutionary approaches, direct search methodologies, or response surface approximations) can be used for this second stage of the optimization.

The information for the sensitivity of the objective function to the design variables available from the SSO stage can be used to readily tune the characteristics of the algorithms used in the second stage. The search may be restricted to I_{SSO}, which is of considerably smaller size (volume) than the original design space Φ. Also, it is established that the sensitivity of the objective function with respect to all components of $\boldsymbol{\varphi}$ is small and, depending on the selection of the shape of admissible subsets, the correlation between design variables may be identified by the orientation and relative scales of the principal axes of I_{SSO} in Φ. This allows for efficient normalization of the design space (in selecting step sizes and blocking criteria), selection of the starting point for iterative algorithms (such as the center $\boldsymbol{\varphi}_{SSO}$), or choice of interpolating functions (for example, for response surface methodologies). Taflanidis and Beck [2] provided more details on how information from SSO can be used to select characteristics (i.e., fine-tune) appropriate stochastic optimization algorithms.

The information from the SSO stage can be additionally exploited to form importance sampling densities for $\boldsymbol{\theta}$. This can be established by using the samples that are available from $\pi(\boldsymbol{\varphi}, \boldsymbol{\theta})$; the $\boldsymbol{\theta}$ component of these samples is distributed proportional to the integrand of the objective function when $\boldsymbol{\varphi} \in I_{\text{SSO}}$. Thus these samples can be used to efficiently create importance sampling densities $p_{\text{IS}}(\boldsymbol{\theta})$ since the set I_{SSO} is small. This last feature is important; it means that the different system configurations compared are not too different and thus the suggested IS densities will be efficient for all of them, i.e., for all $\boldsymbol{\varphi}$ in I_{SSO}. Reference [32] provides an adaptive method for creating such IS densities using samples of the model parameters.

In particular, a combination of SSO with the efficient gradient-based simultaneous-perturbation stochastic approximation (SPSA) [30,33] algorithm has been reported [2,23] to be highly efficient; usually, the second stage requires only a small number of objective function evaluations to converge to the optimal solution. SPSA is an efficient gradient-based algorithm for stochastic search. It uses numerical differentiation, which not only makes it appropriate for complex design problems for which analytic differentiation might be impractical but it also avoids the high computational cost associated with finite difference methods. It is based on the observation that one properly chosen simultaneous random perturbation in all components of $\boldsymbol{\varphi}$ provides as much information for optimization purposes in the long run as a full set of one-at-a-time changes of each component. Thus, it uses only two evaluations of the objective function, in a direction randomly chosen at each iteration, to form an approximation to the gradient vector. It also implements the notion of stochastic approximation, which can significantly improve the computational efficiency of stochastic search methods. This can be established by applying an equivalent averaging across the iterations (by appropriate selection of step sizes) of the algorithm instead of establishing higher accuracy estimates (for the "noisy" objective function) at each iteration. More details about the SPSA algorithm and about how the characteristics of the I_{SSO} set can be used to fine-tune its parameters are provided in the Appendix B. The same sample set $\boldsymbol{\Omega}_{N,k}$ is used in the simulations generating the two different estimates of the objective function at the kth iteration of the optimization algorithm in order to create a consistent estimation error. The principles behind this application are discussed next.

5.3 Common Random Numbers for Stochastic Search. Common random numbers (CRN) provide an efficient methodology for reducing the *relative importance* of the estimation error for the objective function (38) in the stochastic optimization (39). This is established by minimizing the variance between the estimates $\hat{H}(\boldsymbol{\varphi}^1, \boldsymbol{\Omega}_N^1)$ and $\hat{H}(\boldsymbol{\varphi}^2, \boldsymbol{\Omega}_N^2)$, corresponding to two design vectors $\boldsymbol{\varphi}^1$ and $\boldsymbol{\varphi}^2$. This variance can be decomposed as

$$\text{var}(\hat{H}(\boldsymbol{\varphi}^1, \boldsymbol{\Omega}_N^1) - \hat{H}(\boldsymbol{\varphi}^2, \boldsymbol{\Omega}_N^2)) = \text{var}(\hat{H}(\boldsymbol{\varphi}^1, \boldsymbol{\Omega}_N^1)) + \text{var}(\hat{H}(\boldsymbol{\varphi}^2, \boldsymbol{\Omega}_N^2)) - 2\,\text{cov}(\hat{H}(\boldsymbol{\varphi}^1, \boldsymbol{\Omega}_N^1), \hat{H}(\boldsymbol{\varphi}^2, \boldsymbol{\Omega}_N^2)) \tag{46}$$

Adopting common random numbers, i.e., $\boldsymbol{\Omega}_N^2 = \boldsymbol{\Omega}_N^1$, in the simulations generating the two estimates deliberately introduces dependence. This increases the correlation and thus the covariance, which then decreases the variance given by left hand side of Eq. (46). This improves the efficiency of the comparison of the two estimates; it may be equivalently viewed as creating a consistent estimation error. Continuity and monotonicity of the output with respect to the random number input are key issues for improving the efficiency of stochastic comparisons when using common random numbers [34]. If $h(\boldsymbol{\varphi}, \boldsymbol{\theta})$ is sufficiently smooth then these two aforementioned requirements can typically be guaranteed as long as $\|\boldsymbol{\varphi}^1 - \boldsymbol{\varphi}^2\|$ is sufficiently small. For stochastic integrals with discontinuous integrands, such as the use of the indicator function $I_b(.)$ in Eq. (19), efficiency with CRN cannot be guaranteed. It is thus beneficial to use the formulation (22) for the probability of failure in CRN-based optimizations. For design problems in which no model prediction error is actually assumed, a small fictitious error should, therefore, be chosen, especially as optimization problems with and without the model prediction error are often equivalent, i.e., correspond to the same optimum [23].

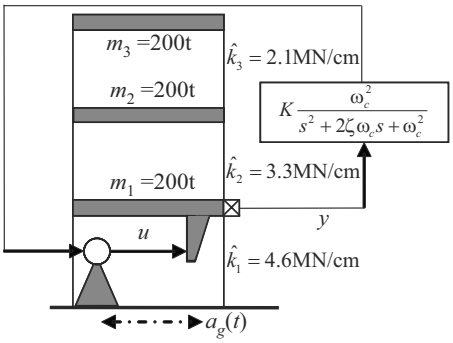

Fig. 3 Structural model

6 Illustrative Example

6.1 Model and Uncertainty Description. The design concepts discussed in this paper are illustrated through a control example concerning the protection of a three-story building against dynamic earthquake excitation. The building is modeled as an ideal three-story shear structure as shown in Fig. 3, which has a state space representation:

$$\dot{\mathbf{x}}_s = \begin{bmatrix} \mathbf{0}_{3\times3} & \mathbf{I}_{3\times3} \\ -\mathbf{M}^{-1}\mathbf{K} & -\mathbf{M}^{-1}\mathbf{Z} \end{bmatrix} \mathbf{x}_s + \begin{bmatrix} \mathbf{0}_{3\times1} \\ \mathbf{E} \end{bmatrix} a_g \tag{47}$$

where $\mathbf{x}_s$ is the structural system state vector, consisting of the displacement and velocities for each floor relative to the ground, a_g is the ground acceleration, the stiffness $\mathbf{K}$, the mass $\mathbf{M}$, and the influence coefficient matrix $\mathbf{E}$ are

$$\mathbf{M} = \begin{bmatrix} 200 & 0 & 0 \\ 0 & 200 & 0 \\ 0 & 0 & 200 \end{bmatrix}, \quad \mathbf{K} = \begin{bmatrix} k_3 & -k_3 & 0 \\ -k_3 & k_2+k_3 & -k_2 \\ 0 & -k_2 & k_1+k_2 \end{bmatrix}, \quad \mathbf{E} = \begin{bmatrix} 1 \\ 1 \\ 1 \end{bmatrix} \tag{48}$$

and damping matrix $\mathbf{Z}$ is chosen so that modal damping of 2% is achieved for all modes of vibration. In Eq. (48), each k_i is the interstory stiffness at floor i and is considered to be uncertain with a nominal value as in Fig. 3. The eigenfrequencies of the nominal structural model are 2.95 Hz, 7.27 Hz, and 11.28 Hz, respectively.

An ideal actuator between the ground and first floor implements a critically damped positive position feedback control law [35] with transfer function:

$$\frac{u(s)}{d_1(s)} = K\frac{\omega_c^2}{s^2 + \sqrt{2}\omega_c + \omega_c^2} \tag{49}$$

where $d_1(.)$ is the relative displacement of the first floor and K and ω_c are design variables.

Performance vector $\mathbf{z}(t)$ consists of seven components: the interstory drift vector $\mathbf{d}(t)$, the absolute story acceleration vector $\mathbf{a}(t)$, and the actuator force $u(t)$. These vectors are nondimensionalized by normalization thresholds of comparable severity, i.e.,

$$\mathbf{z}(t) = \left[\frac{1}{0.01\ \text{m}}\mathbf{d}^T(t) \quad \frac{1}{0.9g}\mathbf{a}^T(t) \quad \frac{1}{5000\ \text{kN}}u(t) \right]^T \tag{50}$$

The chosen earthquake ground excitation model is the stationary response of a modified Kanai–Tajimi filter [36]. The transfer function for this filter is

Table 1 Probability models

Probability model p	Probability distribution
U1	Uniform in $\Theta_c=[0.875\ \ 1.125]$
U2	Uniform in $\Theta_{eq}=[0.917\ \ 1.083]$
G	Gaussian with mean 1 and standard deviation 0.05, truncated within Θ_c

$$H_{wa_g}(s) = \sigma_o \frac{2\zeta_g \omega_g s + \omega_g^2}{(s^2 + 2\zeta_g \omega_g s + \omega_g^2)} \frac{1}{(s+\omega_v)} \tag{51}$$

where ω_g is the characteristic ground motion frequency, $\zeta_g=0.5$ is the damping ratio, and in order to satisfy the condition (A3) in the Appendix A for the absolute acceleration responses, a high-frequency pole $\omega_v=15$ Hz has been introduced compared to the traditional form of the Kanai–Tajimi filter. The gain σ_o is selected so that the RMS intensity of the earthquake input is a_{RMS}.

The structural system (47) is augmented with the excitation model (51) and the compensator (49) to form the closed-loop system. The uncertain model parameters are $\{\omega_g, a_{\mathrm{RMS}}, k_1, k_2, k_3\}$. Each is parameterized by $\omega_g=\theta_g\hat{\omega}_g$Hz, $a_{\mathrm{RMS}}=\theta_R\hat{a}_{\mathrm{RMS}}$ and $k_i=\theta_{s,i}\hat{k}_i$, $i=1,2,3$, where $\hat{\omega}_g$, $\hat{a}_{\mathrm{RMS}}$, and $\hat{k}_i$ denote the most probable values, chosen as 2 Hz, $0.09g$, and the nominal stiffness parameters given in Fig. 3, respectively. The parameters θ_g and θ_R are modeled to be independent uncertain variables while the $\{\theta_{s,i}\}$ are modeled as correlated. The correlation matrix is assumed to be

$$\mathbf{R} = \{\exp[-(j-i)^2/2^2]\} = \begin{bmatrix} 1 & 0.78 & 0.37 \\ & 1 & 0.78 \\ sym & & 1 \end{bmatrix} \tag{52}$$

which implies significant correlation between adjacent stories. Introduction of the linear transformation

$$\boldsymbol{\theta}_{us} = \mathbf{S}^{-1}\boldsymbol{\theta}_s \tag{53}$$

where $\mathbf{S}$ is the lower triangular Cholesky decomposition matrix for $\mathbf{R}$, produces uncorrelated parameters $\{\theta_{us,i}\}$. The set of model parameters for the problem is thus $\boldsymbol{\theta}=[\theta_R\ \ \theta_f\ \ \theta_{us,1}\ \ \theta_{us,2}\ \ \theta_{us,3}]^T$. Each of these parameters is assumed to take values in the range $[0.875\ \ 1.125]$, which creates a compact feasible set Θ_c for the model parameters. However, it should be noted that this methodology can be used for noncompact Θ_c with essentially no added complications. The domain for Φ for the design variables is taken to be $\{K,\omega_c\}=[0,4\cdot10^5]\times[0,40]$.

Three distinct probability models are considered for $\boldsymbol{\theta}$ (Table 1). The first, denoted by U1, assumes a uniform distribution within Θ_c. The second, denoted U2, again assumes a uniform distribution but within the set Θ_{eq} that is defined by the range $[0.917\ \ 1.083]$ for each design variable. The third, denoted G, assumes a truncated Gaussian distribution for each variable with mean value 1 and standard deviation 0.05 and truncated at the boundary of Θ_c. All three probability models have the same mean value. Additionally, G and U2 have the same standard deviation. U1 has larger standard deviation and, thus, may be interpreted as having the largest uncertainty associated with it. This is expected to decrease the overall efficiency of the control application for the performance in U1 since it is more difficult to regulate the response of the system over the larger uncertain parameter space.

These three cases correspond to different prior knowledge for the model parameter values in terms of both the quality and the level of uncertainty. An information-based comparison between them can be established by employing the maximum entropy principle discussed earlier; G would be preferable if we have some knowledge about the mean value and spread (variance) of $\boldsymbol{\theta}$ (assuming we knew that it belonged in Θ_c). Moreover, U1 (or U2) would be appropriate if no prior information is assumed about $\boldsymbol{\theta}$ apart from the fact that it belongs to Θ_c (or Θ_{eq}, respectively).

6.2 Nominal Design. Initially we focus on the nominal model and briefly discuss the comparison between first-passage reliability-based design, $\mathcal{H}_2$ synthesis, and $m\mathcal{H}_2$ synthesis. The controller optimization in this section is performed using the powerful optimization toolbox TOMLAB [37]. For better comparison when presenting the results the controller gain is normalized with respect to the optimal first-passage reliability gain (for the nominal system and $\gamma=1$) and the bandwidth parameter with respect to the fundamental natural frequency of the uncontrolled structure.

The results are presented in Fig. 4 for the nominal design. Part (a) shows the $\mathcal{H}_2$ and $m\mathcal{H}_2$ optimal controllers along with the first-passage reliability optimal controller for different values of the threshold γ. Part (b) shows the probability of failure for the three different design approaches for a time window selection of $T=20$ s and part (c) shows the ratio of the failure rate for optimal $m\mathcal{H}_2$ design over the failure rate for optimal first-passage reliability design. The value of the nondimensional threshold γ is varied

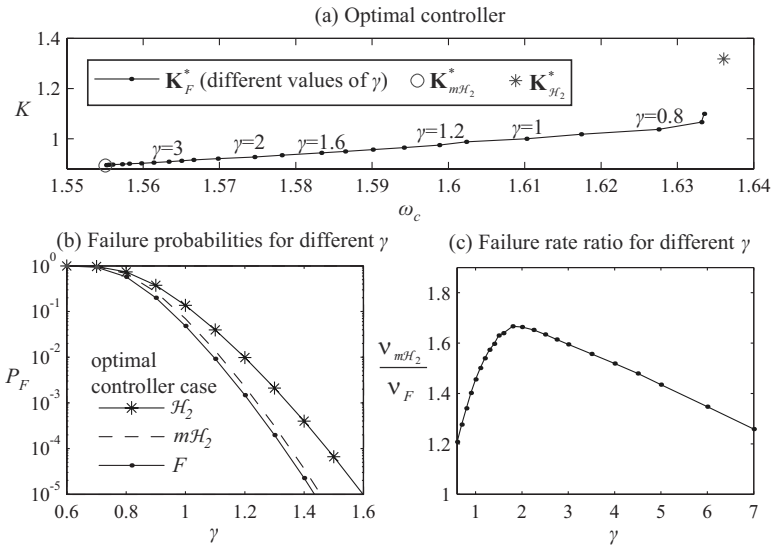

Fig. 4 Comparison between optimal first-passage reliability (labeled *F*), $\mathcal{H}_2$ and $m\mathcal{H}_2$ designs based on nominal model

Table 2 Robust design cases considered

Design	Possibilities for J	Possibilities for p	Robust performance
AR-pJ	$\mathcal{H}_2, m\mathcal{H}_2$	U1, U2, G	Average robustness (probabilistic) for measure J and probability model p
RR-pJ	$m\mathcal{H}_2$	U1, U2, G	Reliability robustness (probabilistic) for measure J and probability model p
FR_c-p	-	U1, U2, G	Robust first-passage reliability for fixed time duration and probability model p
FR-p	-	U1, U2, G	Robust first-passage reliability with uncertain time duration and probability model p
WC-pJ	$\mathcal{H}_2, m\mathcal{H}_2$	Θ_c, Θ_{eq}	Worst case design for measure J for model parameters within p

in the last two plots. The results reported for the optimal first-passage reliability synthesis correspond to the optimal design for the associated value of γ.

As $\gamma \to \infty$, $\mathbf{K}_F^*$ and $\mathbf{K}_{m\mathcal{H}_2}^*$ converge, as do the corresponding failure rates—parts(a) and (c) of Fig. 4. However, the values of P_F at which this convergence becomes apparent represent extremely rare events that are typically of no engineering interest with failure probabilities well below 10^{-4}. For ranges of γ that correspond to more interesting threshold definitions for engineering purposes, there is a significant difference between $\mathbf{K}_F^*$ and $\mathbf{K}_{m\mathcal{H}_2}^*$, as well as their associated first-passage reliability performance.

Even bigger differences exist between $\mathbf{K}_F^*$ and $\mathbf{K}_{\mathcal{H}_2}^*$. These differences become larger as the scaling parameter γ increases, that is, as the performance evaluation focuses more on rare events. This is anticipated as $\mathcal{H}_2$ controllers determine performance based on the Euclidean distance of the response vector, which becomes less related to optimal first-passage reliability as the tails of the distribution for each performance variable become more important.

6.3 Robust Design. We now move on to the robust design. We consider the following design cases: a) Robust first-passage reliability design with either certain or uncertain time duration, denoted by FR_c and FR, respectively, (b) AR for $\mathcal{H}_2$, and (c) both AR and RR for $m\mathcal{H}_2$. For the robust first-passage reliability design γ is set to unity and different values are considered for the time horizon T or its mean value $\bar{T}$ (when considered uncertain). For the RR $m\mathcal{H}_2$ design the threshold b is considered as a scaling of the optimal nominal performance, $b=0.0622\gamma_b$, where 0.0622 is the optimal $m\mathcal{H}_2$ performance for the nominal system and γ_b is the scaling factor that defines the acceptable performance bound relative to that optimal performance.

Apart from the probabilistically robust approaches, the worst-case scenario (denoted WC), a more common notion of feedback robustness, is considered for the $\mathcal{H}_2$ and $m\mathcal{H}_2$ designs. In this case the optimal controller is found by minimizing the maximum of the response measure for model parameters $\boldsymbol{\theta}$ belonging in the compact set Θ_c (or in Θ_{eq} for case U2), i.e.,

$$\mathbf{K}^* = \arg\min_{\mathbf{K}\in\mathcal{K}} \left(\max_{\boldsymbol{\theta}\in\boldsymbol{\Theta}_c} J(\mathbf{K}, \boldsymbol{\theta}) \right) \tag{54}$$

For the controller parameterization considered here, this optimization is nonconvex, and is performed by means of a nonlinear min-max optimization using the TOMLAB optimization toolbox. Table 2 reviews all the robust design cases considered in this study.

The stochastic optimization framework described in Sec. 5 is implemented for the controller design. SSO is applied initially with $N=3000$ samples and selection of admissible subsets as the ellipses that contain 20% of the simulated samples. A direct search algorithm is adopted for optimization (44), again using TOMLAB. The iterative approach in SSO is stopped when $\hat{G}(\hat{I})$ becomes greater than 0.85. A second stage using SPSA with CRN is then applied to converge to the optimal solution within the identified subset in SSO. The size of the sample set for the objective function estimation is set to $N=1000$ and Importance Sampling is implemented, exploiting the information from the last stage of SSO. For the reliability-robustness optimization a small fictitious model prediction error is assumed. This error is taken to be Gaussian-distributed with zero-mean and a standard deviation of 0.02. The limit state function, used in Eq. (22), is defined as

$$g(\mathbf{K}, \boldsymbol{\theta}) = \frac{J(\mathbf{K}|\boldsymbol{\theta})}{b} - 1 \tag{55}$$

We will discuss, separately, the results for the three different performance quantifications considered, starting with $\mathcal{H}_2$ design. The results are reported in Table 3, which shows the optimal controller for the nominal and robust designs along with the performance corresponding to AR, for the three probability models, and WC for Θ_c and Θ_{eq}. The rows of the table correspond to the

Table 3 Optimal design results for $\mathcal{H}_2$ performance

		Optimal K		Optimal-controller performance				
				AR $\mathcal{H}_2$			WC $\mathcal{H}_2$	
		K	ω_c	G	U2	U1	Θ_c	Θ_{eq}
Design approach	Nominal $\mathcal{H}_2$	1.317	1.636	0.255	0.255	0.262	0.698	0.387
	AR-G $\mathcal{H}_2$	1.319	1.606	**0.252**	0.252	0.260	0.635	0.377
	AR-U2 $\mathcal{H}_2$	1.317	1.605	0.252	**0.252**	0.260	0.635	0.377
	AR-U1 $\mathcal{H}_2$	1.317	1.561	0.254	0.254	**0.258**	0.568	0.383
	WC-Θ_c $\mathcal{H}_2$	1.250	1.337	0.264	0.256	0.266	**0.434**	0.366
	WC-Θ_{eq} $\mathcal{H}_2$	1.261	1.418	0.268	0.258	0.270	0.458	**0.358**

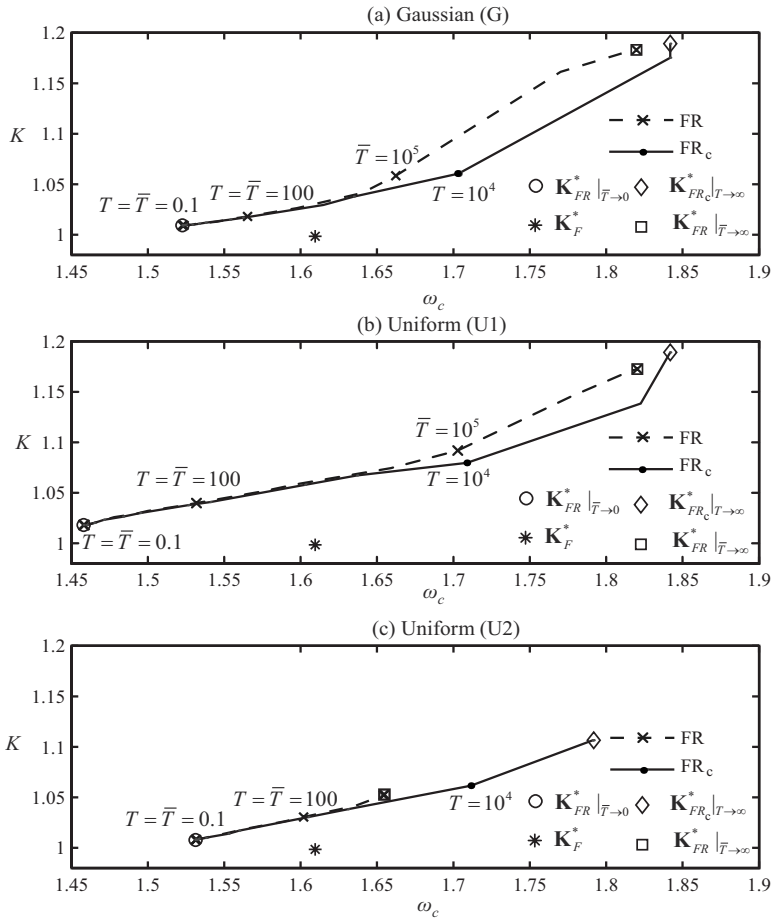

Fig. 5 Optimal first-passage reliability-based controllers

different design approaches and the columns to the different robust-performance quantifications. For each robust-performance quantification, the associated optimal design is in bold. The efficiency of other control synthesis methods with respect to that measure should be judged by comparison to that optimal performance. Small differences exist between the G1 and U2 cases (which correspond to comparable level of uncertainty) for both the optimal controllers as well as their probabilistic performance; this shows that the AR $\mathcal{H}_2$ design and performance are relatively insensitive to the specified probability model. Larger differences exist with respect to the nominal design, as well as the AR $\mathcal{H}_2$-U1, which corresponds to different amount of uncertainty. Also, the optimal attainable performance for U1 is worse, which, as discussed before, is anticipated. The differences in optimal performances and gains between AR and WC designs are much larger. These differences are amplified when the set Θ_c is considered for the possible values for the model parameters, indicating that the worst-case design approach is not appropriate when additional information about these values is available (quantified here by assigning PDFs to them) and when the optimization objective is related to average performance.

Figures 5 and 6 show results for the robust first-passage reliability design. Figure 5 shows the FR and FR_c optimal controllers for various selections of $\bar{T}$ and T, respectively, along with the nominal controller and the controllers corresponding to the three limiting cases given by Eqs. (27), (34), and (33). Results are reported for all three probability models considered. Figure 6 shows the robust first-passage failure probability under optimal design for some of the cases discussed. In Fig. 5, the parameters of the

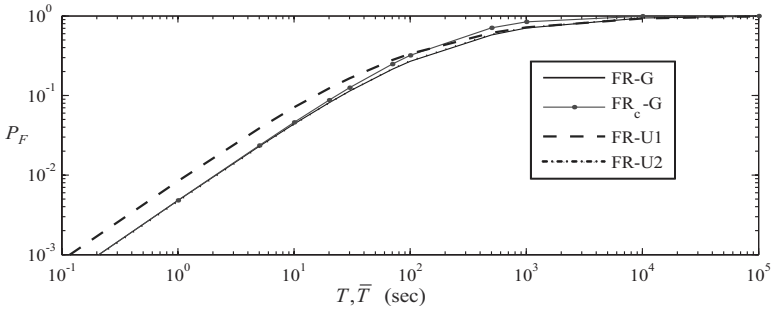

Fig. 6 Failure probability under optimal robust first-passage reliability design

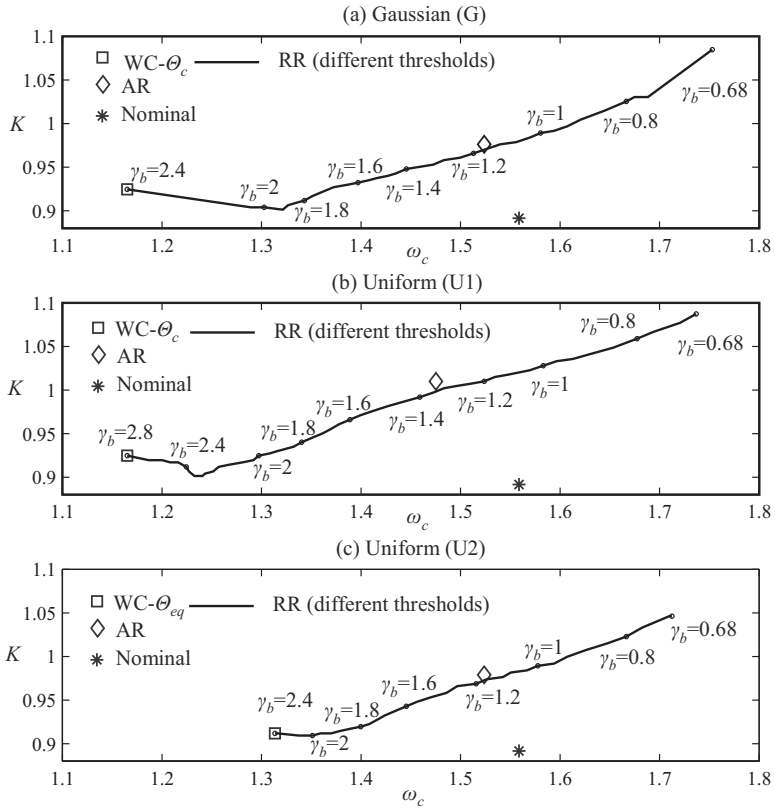

Fig. 7 Optimal controllers for $m\mathcal{H}_2$ synthesis

optimal controller, as T and $\bar{T}$ change, verify the asymptotic behavior predicted in Sec. 4.3. For small time horizons ($\bar{T}$ or T), FR and FR_c designs are practically identical in terms of both the optimal controller and the associated performance and converge to the controller that minimizes the expected out-crossing rate. Only for time horizons above a certain threshold are differences apparent. Comparing the three probability models, the optimal robust-performance for U2 and G is almost identical. The corresponding optimal controllers are different, however, with these differences becoming more pronounced for larger time horizons. Additionally, for large T the optimal FR_c-G controller converges to the FR_c-U1, which is anticipated by the asymptotic result (27) and the fact that the set of possible model parameter values is the same in the two cases. The difference in the plausibility of the different values has no influence in this case. Similar results follow for the FR-G and FR-U1 designs. Considerable differences exist between the designs corresponding to the three probability models, and the optimal controller of the nominal design.

Finally, Figs. 7 and 8 and Table 4 present the results for the $m\mathcal{H}_2$ performance. Figure 7 shows the RR optimal controllers for various thresholds, along with the nominal, AR and WC optimal controllers. Figure 7 shows the RR performance (probability of unacceptable performance) under optimal design as well as for the nominal $m\mathcal{H}_2$ controller. Results are presented for all probability models. Table 4 presents a comparison between nominal, AR and WC designs. The results are reported in similar fashion as in Table 3.

With respect to the RR design, it is evident that as the threshold for acceptable performance increases, the optimal design configuration moves further away from the nominal and the AR designs and it gets closer to a worst-case scenario design approach. Also the sensitivity of the performance objective around that optimal configuration becomes larger. This latter characteristic is obvious when comparing the performances in Fig. 8 and leads to an important implication: for designs problems, where the focus is on rare events, i.e., larger thresholds that determine acceptable system performance, the benefits from using an explicit reliability-based design approach are greater, compared to the designs that consider the nominal or the average performance. The explanation is simple: as the threshold increases, the regions in Θ that simultaneously lead to unacceptable performance *and* have non-negligible probability for the model parameters $p(\boldsymbol{\theta})$ become smaller. Since in reliability context it is only important to regulate the performance in these small regions, the optimal controller can be quite different than the AR one, which focuses on the performance on the average inside Θ, or the nominal one, which only considers the nominal model parameter values. This will occur if these regions are different from the regions for the model parameter values important for the other designs, and ultimately depends on the characteristics of the uncertainty model used, i.e., on the extent of the designer's information about the actual system. Additionally, as the threshold increases the comparative effectiveness of the optimal controller becomes greater because it is easier to

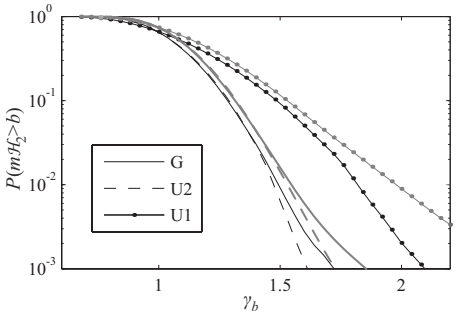

Fig. 8 Probability of unacceptable performance for (*a*) optimal design (black curves) and (*b*) nominal design (grey curves) for different probability models

Table 4 Comparison among nominal, AR, and WC $m\mathcal{H}_2$ designs

		Optimal K		Optimal-controller performance				
				AR $m\mathcal{H}_2$			WC $m\mathcal{H}_2$	
		K	ω_c	G	U2	U1	Θ_c	Θ_{eq}
Design approach	Nominal $m\mathcal{H}_2$	0.892	1.559	0.069	0.069	0.074	0.208	0.119
	AR-G $m\mathcal{H}_2$	0.976	1.524	**0.067**	0.067	0.072	0.222	0.126
	AR-U2 $m\mathcal{H}_2$	0.979	1.524	0.067	**0.067**	0.072	0.222	0.126
	AR-U1 $m\mathcal{H}_2$	1.010	1.475	0.068	0.068	**0.071**	0.210	0.125
	WC-Θ_c $m\mathcal{H}_2$	0.925	1.165	0.075	0.075	0.079	**0.153**	0.116
	WC-Θ_{eq} $m\mathcal{H}_2$	0.912	1.313	0.072	0.072	0.076	0.162	**0.110**

regulate the performance in the smaller regions in the model parameter space that are important for the system reliability. This is expected to lead to greater sensitivity around the optimal solution.

Another interesting discussion of these results is associated with the comparison between the different probability models for the uncertainty quantification. Comparing G and U2, it is evident that small differences exist between the AR performances and similarly for the RR performance when small failure thresholds are considered. However, significant differences in optimal gain and associated optimal performance exist when attention is focused on rare events (large thresholds). Under the probability model G, the probabilities for unacceptable performance are much greater; this indicates that the larger uncertainty, in terms of the information entropy, implied by this probability model is important when considering rare events for the optimal design as well as the associated performance. A similar observation does not hold, especially concerning performance, when the focus is on more frequent failure events. Additionally, the differences reported in Table 4 between the AR $m\mathcal{H}_2$ performances although small, are bigger than the differences for the AR $\mathcal{H}_2$ performance. This indicates that greater sensitivity exists to the specific probability distributions of the parametric model uncertainty for the $m\mathcal{H}_2$ performance for average robustness quantification. The level of uncertainty also has important influence on the design, especially for the RR performance (compare the cases U1 and U2, for example). It is interesting to note that for $\gamma_b=1$, i.e., for a threshold for the acceptable performance equal to the optimal nominal performance, there are minimal differences between the three uncertainty cases, in terms of their optimal performance.

One final comparison is warranted between the two different probabilistic performance quantifications, the AR and the RR. The connection between them, in this example, depends strongly on the definition of acceptable performance. If the focus is on rare events then these design objectives have significantly different characteristics and corresponding optimal design configurations. These remarks illustrate that important differences may exist between the two objectives. Thus, the designer needs to exercise some level of caution when defining the performance measure in the stochastic design framework.

7 Conclusions

The robust stochastic performance optimization of linear time invariant dynamical systems with probabilistically described parametric model uncertainties was discussed in this paper. Both (i) first-passage reliability-based design and (ii) extension of preexisting control methodologies, in particular $\mathcal{H}_2$, and $m\mathcal{H}_2$ synthesis, to account for probabilistic information were considered. The probabilistic design metric was quantified in the latter case either by the average performance over the uncertain parameter space or the probability that the performance will exceed acceptable bounds. Efficient analysis and synthesis methodologies were discussed that are based on stochastic simulation techniques. The control design approach was illustrated in a structural control application. It was demonstrated that even for a design problem with simple dynamics and control law, differences between the optimal first-passage reliability-based design and $\mathcal{H}_2$ or $m\mathcal{H}_2$ synthesis can be important. Additionally, controllers optimized by explicitly considering modeling uncertainties were demonstrated to yield considerable improvement in performance compared to controllers optimized using only a nominal model or by using the more common notion of worst-case robustness. In some applications, this may justify the added computational cost and complexity involved in treating probabilistic performance. Moreover, significant differences were demonstrated to exist for the characteristics of optimal designs, depending on whether the notion of average robustness, as opposed to reliability robustness, was used as an objective function. This is particularly the case when the focus of the latter is on rare events. Reliability robustness was shown to have a strong sensitivity to the level of uncertainty considered, and, when rare events are examined, to the specific probability model adopted to quantify the missing information about the system. Average robustness was found to be insensitive to the probability models considered.

Appendix A: Factors for Stationary Out-Crossing Rate

The factors for the out-crossing rate (13) are discussed in this appendix. Let B_i denote the pair of hyperplanes corresponding to failure mode $i, B_i=\{|z_i|=\gamma\}$. Denoted by Δ_i, the hyperpolygon corresponding to the (n_z-1)-dimensional intersection of S_D and B_i and let $\mathbf{n}_i$ be the unit outward normal vector at the boundary, such that $z_i=\mathbf{n}_i^T\mathbf{z}$, and let $\mathbf{o}_i$ be the orthogonal component of $\mathbf{z}$ such that $\mathbf{o}_i=\mathbf{z}-z_i\mathbf{n}_i$.

Rice's out-crossing rate considers out-crossings over the entire pair of hyperplanes $|z_i|=\gamma$:

$$r_{z_i}^{+}=\lim_{\Delta t\to 0}\frac{E[\text{number of out-crossings in } [t,t+\Delta t] \text{ of } |z_i|=\gamma]}{\Delta t}=\frac{\sigma_{\dot{z}_i}}{\pi\sigma_{z_i}}\exp\left\{-\frac{\gamma^2}{2\sigma_{z_i}^2}\right\} \tag{A1}$$

where $\sigma_{\dot{z}_i}^2$ is the stationary variances for $\dot{z}_i$. Since

$$\dot{\mathbf{z}}(t)=(\mathbf{C}(\boldsymbol{\theta})+\mathbf{D}(\boldsymbol{\theta})\mathbf{KL}(\boldsymbol{\theta}))(\mathbf{A}(\boldsymbol{\theta})+\mathbf{B}(\boldsymbol{\theta})\mathbf{KL}(\boldsymbol{\theta}))\mathbf{x}(t)+(\mathbf{C}(\boldsymbol{\theta})+\mathbf{D}(\boldsymbol{\theta})\mathbf{KL}(\boldsymbol{\theta}))\mathbf{E}\mathbf{w}(t) \tag{A2}$$

and $\mathbf{w}(t)$ is white noise, it follows that for the problem to be well-posed, i.e., for $\sigma_{\dot{z}_i}^2$ to be finite, the following relationship needs to hold:

$$(\mathbf{C}(\boldsymbol{\theta})+\mathbf{D}(\boldsymbol{\theta})\mathbf{KL}(\boldsymbol{\theta}))\mathbf{E}=0, \quad \forall\ \mathbf{K}\in\mathcal{K} \tag{A3}$$

This restriction is equivalent to the requirement that the response vector $\mathbf{z}(t)$ be differentiable. Given that Eq. (A3) holds we have

$$\sigma_{\dot{z}_i}^2=\mathbf{n}_i^T[(\boldsymbol{\theta})\mathbf{C}+\mathbf{D}(\boldsymbol{\theta})\mathbf{KL}(\boldsymbol{\theta})][\mathbf{A}(\boldsymbol{\theta})+\mathbf{B}(\boldsymbol{\theta})\mathbf{KL}(\boldsymbol{\theta})]\boldsymbol{\Phi}[\mathbf{A}(\boldsymbol{\theta})+\mathbf{B}(\boldsymbol{\theta})\mathbf{KL}(\boldsymbol{\theta})]^T[\mathbf{C}(\boldsymbol{\theta})+\mathbf{D}(\boldsymbol{\theta})\mathbf{KL}(\boldsymbol{\theta})]^T\mathbf{n}_i \tag{A4}$$

The correlation weighting factor θ_{z_i} corresponds to the (n_z-1)-dimensional integral:

$$\theta_{z_i} = P[\boldsymbol{o}_i \in \Delta_i | |z_i| = \gamma] = \int_{\Delta_i} p(\boldsymbol{o}_i | |z_i| = \gamma) d\boldsymbol{o}_i \tag{A5}$$

For the evaluation of this multidimensional integral, note first that the probability density $p(\mathbf{o}_i | |z_i| = \gamma)$ is Gaussian with mean and covariance matrix, which are algebraically related to $\mathbf{\Phi}$ (see, for example, Ref. [38]). Genz [39] proposed a highly efficient algorithm for evaluation of such multidimensional Gaussian integrals.

Finally, λ_{z_i} is a temporal correlation adjustment to account for the conditioning of the out-crossing rate $\nu_{\mathbf{z}}^{+}$ on the absence of prior out-crossings, as in Eq. (12). Neglecting this factor is equivalent to assuming a Poisson process approximation for the out-crossing events (i.e., independence between out-crossings) and this assumption may not be justified for narrow-band systems, as well as for small failure thresholds. Many semi-empirical approximations exist for this correction factor. The following approximation by Taflanidis and Beck [19] was shown to exhibit a great deal of flexibility with respect to the dynamic system bandwidth characteristics:

$$\lambda_{z_i} \approx \frac{1 - \exp\left\{ -q^{0.6} \left(\frac{2}{\sqrt{\pi}} \right)^{0.2} \frac{\gamma\sqrt{2}}{\sigma_{z_i}} \right\}}{1 - \exp(-\gamma^2/(2\sigma_{z_i}^2))}, \quad q = \frac{\sigma_{z_i}^6}{4\pi I_{ce} I_{cv}} \tag{A6}$$

where for a process with spectral density $S_{z_i z_i}$: $I_{cv} = \int_{-\infty}^{\infty} |\omega| S_{z_i z_i}(\omega) d\omega$ and $I_{ce} = \int_{-\infty}^{\infty} S_{z_i z_i}^2(\omega) d\omega$. These two integrals may be numerically evaluated by substituting the spectral density $S_{z_i z_i}$ for the equivalent expression $\mathbf{H}_{z_i}(\omega)\mathbf{H}_{z_i}(\omega)^*/(2\pi)$, where $\mathbf{H}_{z_i}(\omega)$ is the transfer function for z_i:

$$\mathbf{H}_{z_i}(\omega) = \mathbf{n}_i^T \mathbf{C}(\boldsymbol{\theta}) [i\omega \mathbf{I} - \mathbf{A}(\boldsymbol{\theta})]^{-1} \mathbf{E}(\boldsymbol{\theta}) \tag{A7}$$

Appendix B: Stochastic Perturbation Simultaneous Approximation With Common Random Numbers

The implementation of SPSA takes the iterative form

$$\boldsymbol{\varphi}_{k+1} = \boldsymbol{\varphi}_k - \alpha_k \mathbf{g}_k(\boldsymbol{\varphi}_k, \mathbf{\Omega}_{N,k}) \tag{B1}$$

where $\boldsymbol{\varphi}_1 \in \Phi$ is the chosen point to initiate the algorithm and the jth component for the CRN simultaneous perturbation approximation to the gradient vector in the kth iteration, $\mathbf{g}_k(\boldsymbol{\varphi}_k, \mathbf{\Omega}_{N,k})$, is given by

$$g_{k,j} = \frac{\hat{H}(\boldsymbol{\varphi}_k + c_k \Delta_k, \mathbf{\Omega}_{N,k}) - \hat{H}(\boldsymbol{\varphi}_k - c_k \Delta_k, \mathbf{\Omega}_{N,k})}{2 c_k \Delta_{\kappa,j}} \tag{B2}$$

$\Delta_k \in \mathbb{R}^{n_\varphi}$ in Eq. (B2) is a vector of mutually independent random variables that defines the random direction of simultaneous perturbation for $\boldsymbol{\varphi}_k$ and that satisfies the statistical properties given in Ref. [30]. A symmetric Bernoulli ± 1 distribution is typically chosen for the components of Δ_k. The selection for the sequences $\{c_k\}$ and $\{\alpha_k\}$ is discussed in detail in Ref. [33]. A choice that guarantees asymptotic convergence to $\boldsymbol{\varphi}^*$ is $\alpha_k = \alpha/(k+w)^\beta$ and $c_k = c_1/k^\zeta$, where $4\zeta - \beta > 0$, $2\beta - 2\zeta > 1$ with w, $\zeta > 0$, and $0 < \beta \leq 1$. Regarding the rest of the parameters for the sequences $\{c_k\}$ and $\{\alpha_k\}$: w is typically set to 10% of the number of iterations selected for the algorithm and the initial step c_1 is chosen "close" to the standard deviation of the initial estimation error, i.e. for $\boldsymbol{\varphi}_1$. Convergence of the iterative process is judged based on the value $\|\boldsymbol{\varphi}_{k+1} - \boldsymbol{\varphi}_k\|$ in the last few steps, for an appropriate selected vector norm. Blocking rules can also be applied in order to avoid potential divergence of the algorithm, especially in the first iterations (see Ref. [30] for more details). The following guidelines can be used for tuning of the SPSA parameters using information from SSO [2]: $\boldsymbol{\varphi}_1$ should be selected as the center of the set I_{SSO} and parameter a can be chosen so that the initial step for each component of $\boldsymbol{\varphi}$ is smaller than a certain fraction (chosen as 1/10) of the respective size of I_{SSO}, based on the estimate for $\mathbf{g}_1$ from Eq. (B2). This estimate should be averaged over n_g (chosen as 6) evaluations because of its importance in the efficiency of the algorithm. Also, no movement in any direction should be allowed that is greater than a quarter of the size of the respective dimension of I_{SSO} (blocking rule).

References

[1] Jaynes, E. T., 2003, *Probability Theory: The Logic of Science*, Cambridge University Press, Cambridge, UK.

[2] Taflanidis, A. A., and Beck, J. L., 2008, "An Efficient Framework for Optimal Robust Stochastic System Design Using Stochastic Simulation," Comput. Methods Appl. Mech. Eng., **198**(1), pp. 88–101.

[3] Stengel, R., and Ray, L., 1991, "Stochastic Robustness of Linear Time-Invariant Control Systems," IEEE Trans. Autom. Control, **36**(1), pp. 82–87.

[4] Dullerud, G. E., and Paganini, F., 1999, *A Course in Robust Control Theory: A Convex Approach*, Springer-Verlag, New York.

[5] Zhou, K., and Doyle, J. C., 1997, *Essentials of Robust Control*, Prentice Hall, Upper Saddle River, NJ.

[6] Stengel, R., Ray, L., and Marrison, C., 1995, "Probabilistic Evaluation of Control-System Robustness," Int. J. Syst. Sci., **26**(7), pp. 1363–1382.

[7] Ray, L. R., and Stengel, R. F., 1992, "Stochastic Measures of Performance Robustness in Aircaft Control Systems," J. Guid. Control Dyn., **15**(6), pp. 1381–1387.

[8] Wang, Q., and Stengel, R. F., 2002, "Robust Control of Nonlinear Systems With Parametric Uncertainty," Automatica, **38**(9), pp. 1591–1599.

[9] Boers, Y., Weiland, S., and Damen, A. A. H., 1997, "Expected $\mathcal{H}_2$ Performance Control for Systems With Statistical Uncertainty," American Control Conference, Albuquerque, NM, pp. 1225–1229.

[10] Boers, Y., 2002, "Average Performance Control by Static Output Feedback," IEE Proc.: Control Theory Appl., **149**(3), pp. 188–192.

[11] Field, R. V. J., Voulgaris, P. G., and Bergman, L. A., 1996, "Methods to Compute Probabilistic Measures of Robustness for Structural Systems," J. Vib. Control, **2**(4), pp. 447–463.

[12] May, B., and Beck, J., 1998, "Probabilistic Control for the Active Mass Driver Benchmark Structural Model," Earthquake Eng. Struct. Dyn., **27**(11), pp. 1331–1346.

[13] Yuen, K., and Beck, J., 2003, "Reliability-Based Robust Control for Uncertain Dynamical Systems Using Feedback of Incomplete Noisy Response Measurements," Earthquake Eng. Struct. Dyn., **32**(5), pp. 751–770.

[14] Taflanidis, A. A., Scruggs, J. T., and Beck, J. L., 2008, "Reliability-Based Performance Objectives and Probabilistic Robustness in Structural Control Applications," J. Eng. Mech., **134**(4), pp. 291–301.

[15] Levine, W., and Athans, M., 1970, "On the Determination of the Optimal Constant Output Feedback Gains for Linear Multivariable Systems," IEEE Trans. Autom. Control, **15**(1), pp. 44–48.

[16] Syrmos, V. L., Abdallah, C. T., Dorato, P., and Grogoriadis, K., 1997, "Static Output Feedback—A Survey," Automatica, **33**(2), pp. 125–137.

[17] Goh, K. C., Safonov, M. G., and Papavassilopoulos, G. P., 1994, "A Global Optimization Approach for the BMI Problem," Thirty-Third IEEE Conference on Decision and Control, Vol. 3, pp. 2009–2014.

[18] Camino, J. F., Oliveira, M. C., and Skelton, R. E., 2000, "A Convexifying Algorithm for the Design of Structured Linear Controllers," Thirty-Ninth IEEE Conference on Decision and Control, Sydney, Australia, pp. 2781–2786.

[19] Taflanidis, A. A., and Beck, J. L., 2006, "Analytical Approximation for Stationary Reliability of Certain and Uncertain Linear Dynamic Systems With Higher Dimensional Output," Earthquake Eng. Struct. Dyn., **35**(10), pp. 1247–1267.

[20] Taflanidis, A. A., 2010, "Reliability-Based Optimal Design of Linear Dynamical Systems Under Stochastic Stationary Excitation and Model Uncertainty," Eng. Struct., **32**(5), pp. 1446–1458.

[21] Beck, J. L., and Katafygiotis, L. S., 1998, "Updating Models and Their Uncertainties. I: Bayesian Statistical Framework," J. Eng. Mech., **124**(4), pp. 455–461.

[22] Shannon, C. E., 1948, "A Mathematical Theory of Communications," Bell Syst. Tech. J., **27**, pp. 279–343 and 623–656.

[23] Taflanidis, A. A., and Beck, J. L., 2008, "Stochastic Subset Optimization for Optimal Reliability Problems," Probab. Eng. Mech., **23**(2–3), pp. 324–338.

[24] Robert, C. P., and Casella, G., 2004, *Monte Carlo Statistical Methods*, Springer, New York, NY.

[25] Calafiore, G., and Dabbene, F., 2002, "A Probabilistic Framework for Problems With Real Structured Uncertainty in Systems and Control," Automatica, **38**(8), pp. 1265–1276.

[26] Berg, B. A., 2004, *Markov Chain Monte Carlo Simulations and Their Statistical Analysis*, World Scientific, Singapore.

[27] Calafiore, G., Dabbene, F., and Tempo, R., 2007, "A Survey of Randomized Algorithms for Control Synthesis and Performance Verification," J. Complex., **23**(3), pp. 301–316.

[28] Polak, E., and Royset, J. O., 2008, "Efficient Sample Size in Stochastic Nonlinear Programming," J. Comput. Appl. Math., **217**(2), pp. 301–310.

[29] Ruszczynski, A., and Shapiro, A., 2003, *Stochastic Programming*, Elsevier, New York.
[30] Spall, J. C., 2003, *Introduction to Stochastic Search and Optimization*, Wiley-Interscience, New York.
[31] Taflanidis, A. A., 2007, "Stochastic System Design and Applications to Stochastically Robust Structural Control," Ph.D. thesis, California Institute of Technology, Pasadena.
[32] Au, S. K., and Beck, J. L., 1999, "A New Adaptive Importance Sampling Scheme," Struct. Safety, **21**(2), pp. 135–158.
[33] Kleinman, N. L., Spall, J. C., and Naiman, D. C., 1999, "Simulation-Based Optimization With Stochastic Approximation Using Common Random Numbers," Manage. Sci., **45**(11), pp. 1570–1578.
[34] Glasserman, P., and Yao, D. D., 1992, "Some Guidelines and Guarantees for Common Random Numbers," Manage. Sci., **38**(6), pp. 884–908.
[35] Fanson, J. L., and Caughey, T. K., 1990, "Positive Position Feedback Control for Large Space Structures," AIAA J., **28**(4), pp. 717–724.
[36] Clough, R. W., and Penzien, J., 1993, *Dynamics of Structures*, McGraw-Hill, New York, NY.
[37] Holmstrom, K., Goran, A. O., and Edvall, M. M., 2007, "User's Guide for Tomlab 5.8," Tomlab Optimization Inc., www.TOMLAB.biz, San Diego, CA.
[38] Johnson, R. A., and Wichern, D. W., 2002, *Applied Multivariate Statistical Analysis*, Prentice Hall, Upper Saddle River, NJ.
[39] Genz, A., 1992, "Numerical Computation of Multivariate Normal Probabilities," J. Comput. Graph. Stat., **1**(2), pp. 141–149.